SUBSURFACE MAPPING OF RUSTENBURG LAYERED SUITE (RLS), BUSHVELD COMPLEX, SOUTH AFRICA: INFERRED STRUCTURAL FEATURES USING BOREHOLE DATA AND SPATIAL ANALYSIS

O.A. Bamisaiye[a, *], P.G. Eriksson[a], J.L. Van Rooy[a], H.M. Brynard[b], S.Foya[b], A.Y. Billay[b], V. Nxumalo[b]

[a] Department of Geology, University of Pretoria, Private Bag X20 Hatfield, Pretoria, 0028, South Africa

[b] Council for Geoscences, Pretoria, South Africa

*Corresponding author. adunseyi@gmail.com (O.A. Bamisaiye).

Highlights

- Unsubstantiated inferences about the RLS subsurface structures are made evident.
- Possible magma transport direction are highlighted.
- A summary of the major structural trends and their interpretations is given.
- Better understanding of local and regional structural trends is provided.
- A new way of mapping subsurface geological features in detail is provided.

ABSTRACT

Faults and other structural features within the mafic-ultramafic layers of the Bushveld Complex have been a major issue mainly for exploration and mine planning. This study employed a new approach in detecting faults with both regional and meter scale offsets, which was not possible with the usually applied structure contour mapping. Interpretations of faults from structural and

isopach maps were previously based on geological experience, while meter-scale faults were virtually impossible to detect from such maps. Spatial analysis was performed using borehole data primarily. This resulted in the identification of previously known structures and other hitherto unsuspected structural features. Consequently, the location, trends, and geometry of faults and some regional features within the Rustenburg Layered Suite (RLS) that might not be easy to detect through field mapping are adequately described in this study.

Keywords: spatial analysis, structural map, isopach maps, faults, folds, Rustenburg Layered Suite.

1. INTRODUCTION

Structure contours and isopach patterns can be used to delineate folds, faults and other structural features (Jones et al., 2008; Cant, 1988; Barclay et al., 1990). Detection of regional structural trend and fault offset with the use of structure contours and isopach maps had been widely applied for almost half a century by various workers in exploration research (Cant, 1988; Barclay et al., 1990; Cather and Harrison, 2002; Roberts, 2003; Xu et al. ,2004; Groshong, 2006; Mei, 2009). Extensive exploration and mining for PGM and chrome within the world famous Rustenburg Layered Suite of the Bushveld Complex has contributed immensely to knowledge about major and minor surface structures within the area. Information from mine plans has permitted more detailed mapping of some of these faults at local scale. Most of the earlier studies (Van Der Merwe, 1978; Meyer and De Beer, 1987; Du Plessis and Walraven, 1990; Bumby et al., 1998; Friese and Chunnett, 2004; Nex, 2005) are limited to observation of structural features at the surface or features exposed by mining activities close to the surface. Usually such

structures are identified using magnetic (Campbell, 2011), aeromagnetic (Cole, 2013; Campbell, 2006; Campbell , 2011), gravity (Campbell, 2011; Du Plessis and Kleywegt, 1987), and seismic data (Du Plessis and Levitt, 1987; Odgers et al., 1993; Odgers, 1998; Trickett et al., 2005; Campbell, 2006; Campbell, 2009). More detailed studies on the nature of these structures are, however, confined to several meters below the sub-surface. The purpose of this paper is to analyse available borehole data for accurate interpretation of subsurface features and to determine the nature and age relationship of faults and other features that might not be apparent at the surface, through the correlation of stratigraphic horizons and detailed structural interpretation. This paper thus describes the location, trends, and geometry of faults and some regional features within the Rustenburg Layered Suite (RLS) that might not be easy to detect during field mapping. Spatial analysis was performed using borehole data. Many of the borehole logs provide lithostratigraphic information of horizons that can be correlated continuously across the lobes of the Bushveld Complex.

2. STRUCTURAL FEATURES IN THE BUSHVELD COMPLEX

The Bushveld Complex (BC) is located in the northern parts of South Africa and eastern Botswana (Figure 1A). It outcrops as northern, western, eastern, far western and far northern lobes. Previous researchers (e.g., Van Der Merwe, 1978; Du Plessis and Walraven, 1990; Friese and Chunnett, 2004; Nex, 2005) identified numerous faults in the RLS of the northern lobe. Some of these faults include: the regional ENE trending faults parallel to the Palala Shear Zone and the Thabazimbi Murchison Lineament (TML: du Plessis & Walraven 1990) (Figure 1); NNE-NE trending faults associated with the tectonic movement along the NE trending structures; the later East-West trending structures and the earliest N-S trending structures formed during the emplacement of the Bushveld Complex (Hulbert, 1983). NW-NNW and NE-SW

A

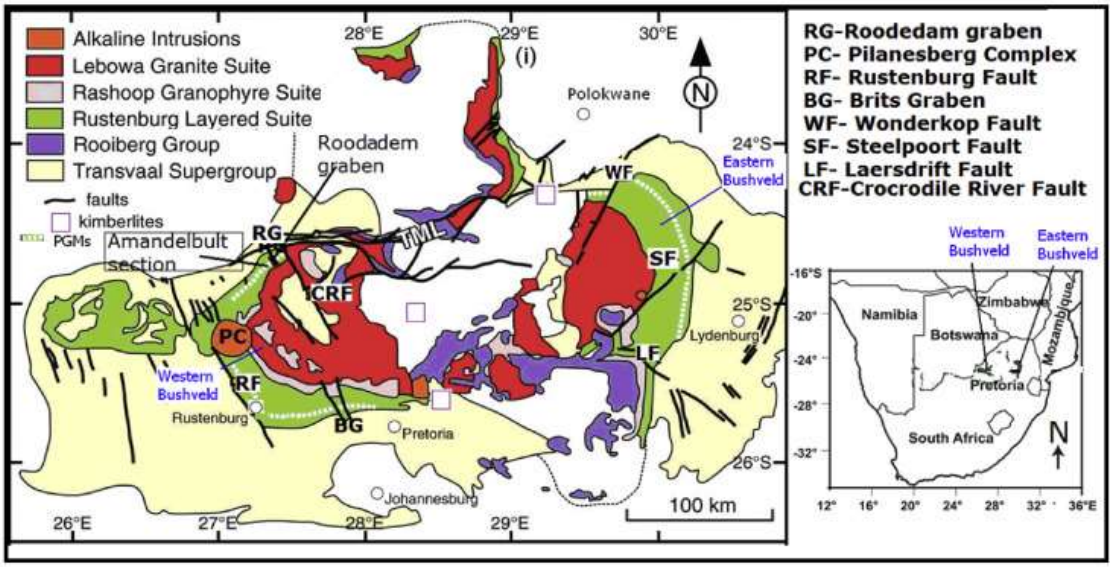

B

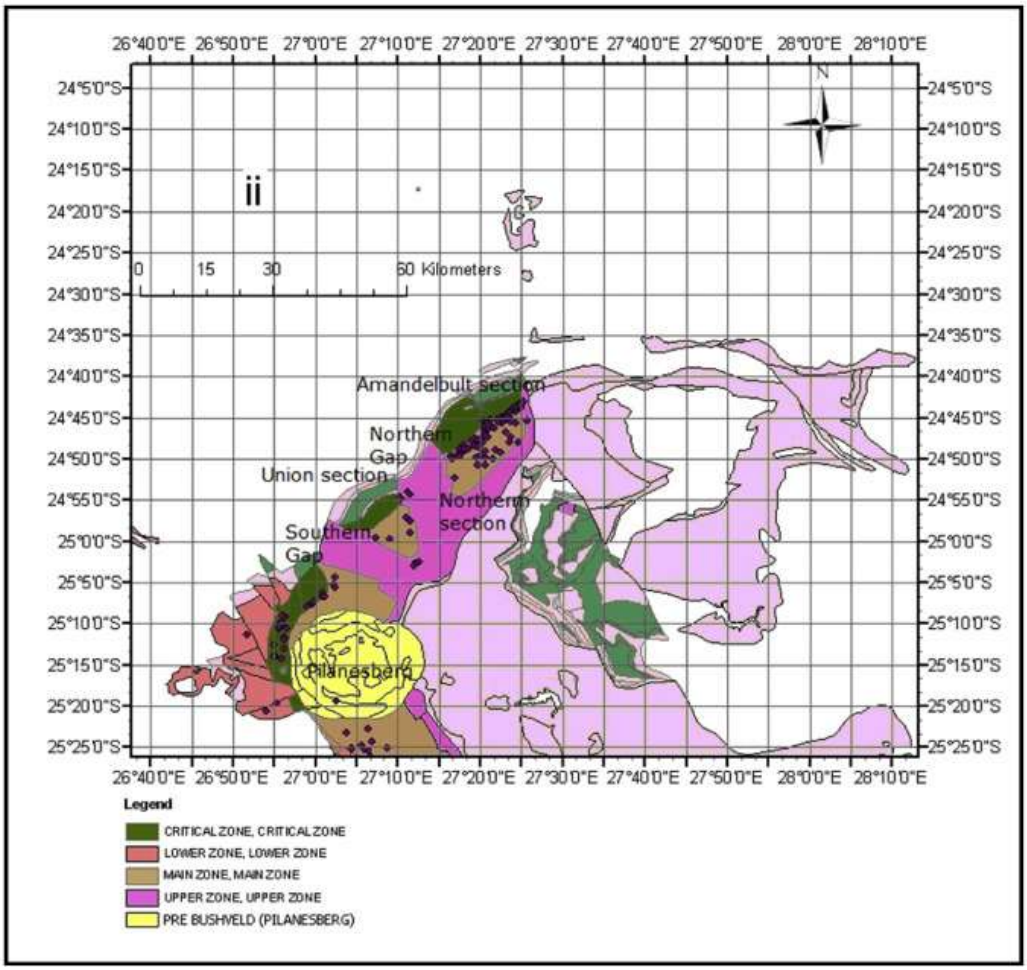

Fig. 1. (A): Geological map of the Bushveld Complex. Modified after Scoates and Friedman (2008).
B: Geological map of the western Bushveld showing the areas mentioned in text.

trending structures are common in the Western Bushveld lobe (Vermaak, 1976; Bumby et al., 1998). Ductile deformation of the floor rocks, especially in the Eastern Bushveld lobe resulted in folding and diapirism (Uken and Watkeys, 1997; Clarke et al., 2005; Clarke et al., 2009) while initial brittle deformation resulted in 'stepped and fingered intrusion' patterns (Clarke et al., 2009). Folding initiated by bending of the original horizontally layered suite resulted in the development of layer parallel faults, duplexes and formation of the present basin-fold geometry of the Bushveld Complex (Perritt and Roberts, 2007).

3. METHODS

More than 1200 borehole-log obtained from the files of the Council for Geoscience (CGS) in Pretoria, South Africa were collated and analysed by contouring the elevation at each stratigraphic contact. Interval structure contour maps for the top and base of each stratigraphic unit were constructed using Kriging and Trend Surface Residual interpolation methods in a Rockwoks®15 environment. The interval isopach maps were generated by subtracting the lower contact elevation of each stratigraphic contact from the upper or top elevation, taking the orientation of each well and collar elevation into consideration. These were augmented with available geophysical data (aeromagnetic and seismic) and field reports.

The structural mapping was based on interpretation of interval structural contour maps, thickness variation, shaded relief, structural profiles (used to measure offset on interval structure and isopach maps) and information about existing structural styles in the area. Geometric interpretation was based on change in depth, curvature, structural highs (peaks, maxima or ridges) and lows (depressions, trenches or valleys), nature of slope on interval structure contours

and interval isopach maps (cf., Prost, 2004). The major focus was on the trend of closely spaced contours and the undulations on interval structure contour maps. Integration of existing fault surfaces with interval structure contours and thickness maps at different horizons was carried out in order to better understand the geometry of the underlying structure. Profiles drawn across the stratigraphic interval structure contours accurately depicted the exact location, offset and geometry of faults. Image processing techniques such as slope analysis and shaded relief enhanced visual interpretation of the linear offsets (Mossop and Shetsen, 1994). Three-dimensional models were used to relate the displacement of a stratigraphic unit to its up-throw and down-dipping direction along the fault planes. Interpretation of faults from structural contours and thickness maps was based on the following:

- Abrupt change in elevation of stratigraphic top, along a linear pattern is interpreted as a fault.
- Close observation of tight isolines.
- Repetition of similar or the same offset pattern on several successive stratigraphic units.
- Deviation of isolines from the regional trend most especially on interval isopach maps.
- Normal faults thin the stratigraphy and usually dip towards the thicker end while reverse faults thicken the stratigraphy and dip away from the thicker side of a specific unit.
- Reef delineation from geophysical data is often based on the presence of faults inferred from specific magnetic, density, refraction or any other physical contrast. However, reefs are clearly delineated from borehole data. The reef top and floor boundaries were delineated by picking the top and base of each contact from borehole log data.

4. RESULTS

The geology of the Bushveld Complex showing the lithologic distribution around the BC is shown in Figure 1A. Each lobe of the Bushveld Complex is subdivided into sections (Figure 1B, Figure 5B, Figure 12A and Figure 19A) to enhance detailed description.

4.1 Structures in the Northwestern Bushveld

A NW-SE structural trend is prominent around the Amandelbult section (Figures 1A, 2A and 2B) while NNW and NW trends dominate the central part of the Northwestern Bushveld (i.e from the northern gap area through the Union section to the southern gap area; Figures 3A, 3B, 4A, and 4B). The Upper Zone interval structural contour map through to the Lower Zone structural contour interval show a successive NNW and NE trend at the centre. However, the NNW trend is more prominent on the Upper Zone interval structural contour map (Figure 2A), while the NE trend is dominant from the Main Zone to the Lower Zone interval structural contour maps as illustrated in the rose diagram (Figure 2E). The NE trend cuts across the NNW trend (Figures 2A, 2B, 2C and 2D). This indicates that the NE structural trend might be younger than the NNW trend.

The NW–SE structural trend coincides with the trend of the Roodedam graben located in Middellaagte farm at the NE part of the Northwestern Bushveld Complex. The Roodedam/Middellaagte Graben also coincides with a central depression (downthrown part) bounded by two faults (Figures 2C and 2D). The bounding faults are closer at the north and widen southward dipping away from each other on the interval structure contour maps. This graben structure is probably a pre-Bushveld feature since the interval structural contour map (Figure 2C) and isopach map (Figure 2D) indicate an inverse relationship. This means that areas

A

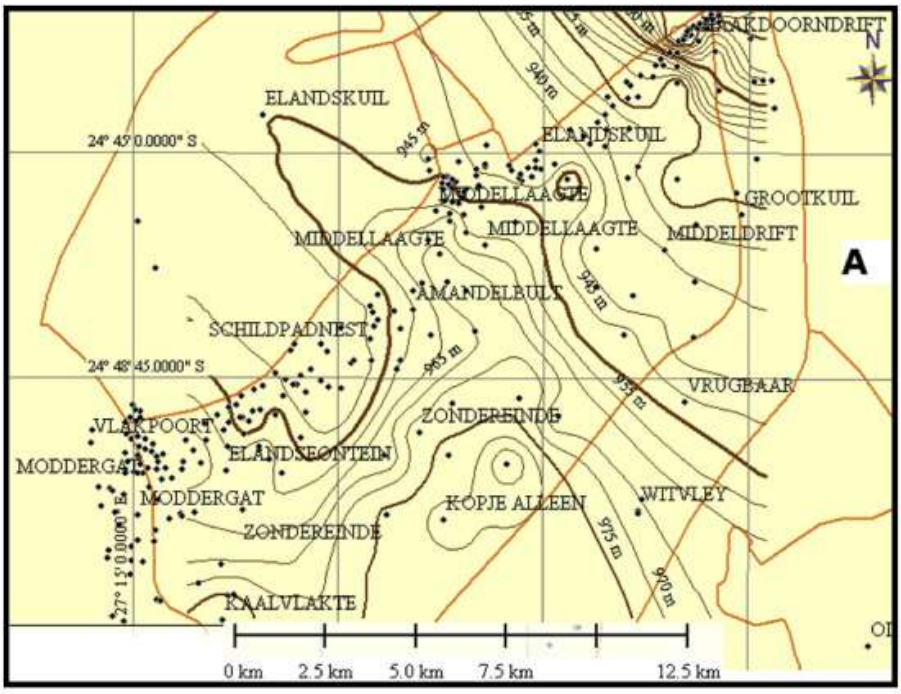
HAAKDOORNDRIFT
N
ELANDSKUIL
24° 45' 0.0000" S
945 m
ELANDSKUIL
MIDDELLAAGTE
GROOTKUIL
MIDDELLAAGTE
MIDDELLAAGTE
MIDDELDRIFT
A
AMANDELBULT
945 m
SCHILDPADNEST
24° 48' 45.0000" S
985 m
955 m
VRUGBAAR
ZONDEREINDE
VLAKPOORT
ELANDSFONTEIN
MODDERGAT
MODDERGAT
KOPJE ALLEEN
WITVLEY
975 m
ZONDEREINDE
27° 15' 0.0000" E
970 m
KAALVLAKTE
0 km
2.5 km
5.0 km
7.5 km
12.5 km

B

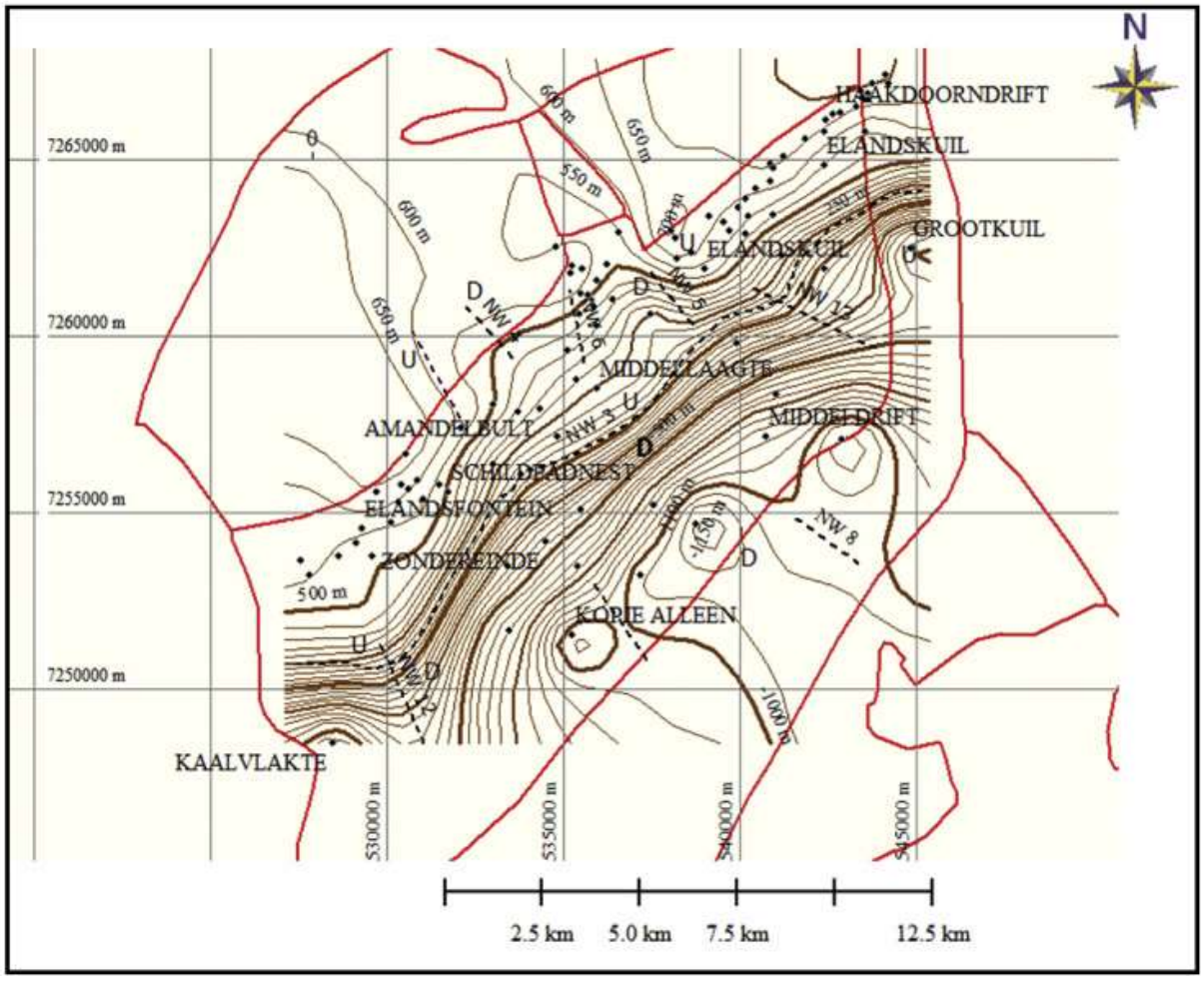
N
HAAKDOORNDRIFT
600 m
650 m
ELANDSKUIL
7265000 m
550 m
GROOTKUIL
ELANDSKUIL
600 m
D
NW
650 m
U
7260000 m
MIDDELLAAGTE
AMANDELBULT
MIDDELDRIFT
SCHILDPADNEST
7255000 m
ELANDSFONTEIN
ZONDEREINDE
500 m
KOPJE ALLEEN
7250000 m
KAALVLAKTE
530000 m
535000 m
540000 m
545000 m
2.5 km
5.0 km
7.5 km
12.5 km

c

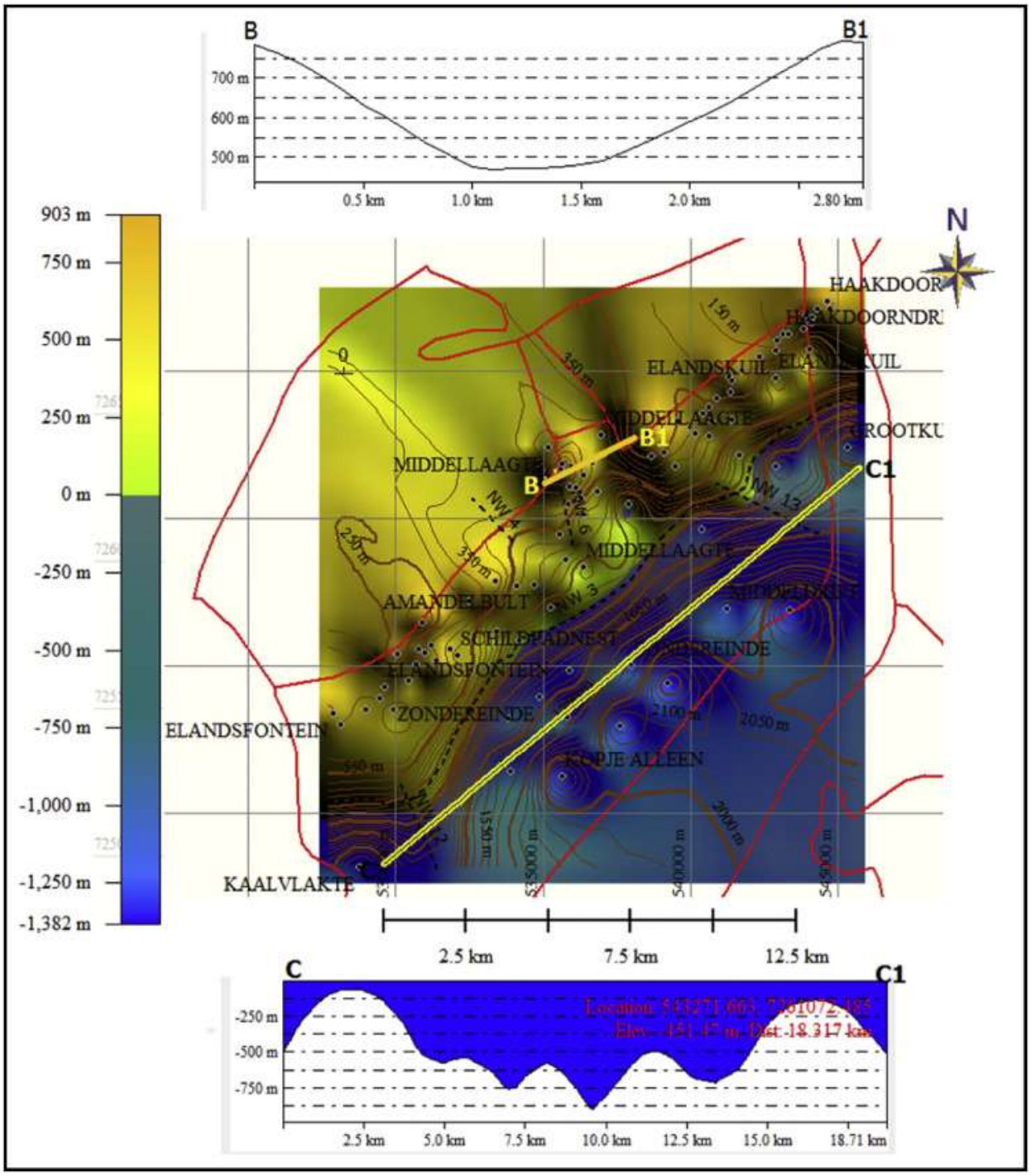
B
B1
700 m
600 m
500 m
0.5 km
1.0 km
1.5 km
2.0 km
2.80 km
903 m
750 m
500 m
250 m
0 m
-250 m
-500 m
-750 m
-1,000 m
-1,250 m
-1,382 m
N
HAAKDOORN
HAAKDOORNDR
ELANDSKUIL
ELAN KUIL
GROOTKU
MIDDELLAAGTE
MIDDELLAAGTE
B1
B
C1
AMANDELBULT
SCHILPADNEST
ELANDSFONTEIN
ZONDEREINDE
ELANDSFONTEIN
ZONDEREINDE
KOPJE ALLEEN
KAALVLAKTE
150 m
350 m
250 m
350 m
NW 4
NW 6
NW 3
NW 13
1600 m
2100 m
2050 m
2000 m
1550 m
540 m
S3500 m
S4000 m
S4500 m
2.5 km
7.5 km
12.5 km
C
C1
-250 m
-500 m
-750 m
2.5 km
5.0 km
7.5 km
10.0 km
12.5 km
15.0 km
18.71 km

D

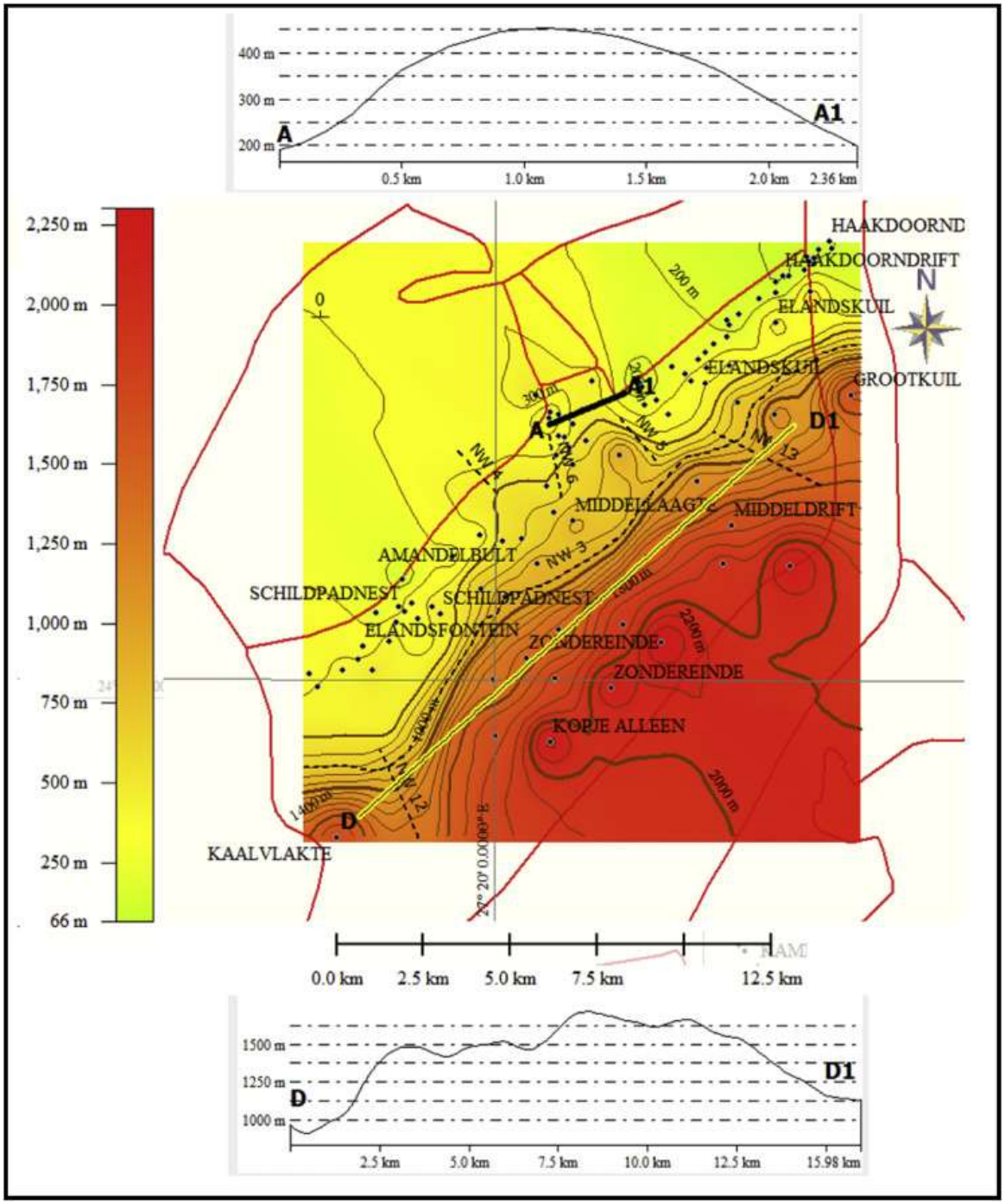
400 m
300 m
200 m
A
A1
0.5 km
1.0 km
1.5 km
2.0 km
2.36 km
2,250 m
2,000 m
1,750 m
1,500 m
1,250 m
1,000 m
750 m
500 m
250 m
66 m
HAAKDOORND
HAAKDOORNDRIFT
N
ELANDSKUIL
ELANDSKUIL
GROOTKUIL
D1
MIDDELLAAGTE
MIDDELDRIFT
AMANDELBULT
SCHILDPADNEST
SCHILDPADNEST
ELANDSFONTEIN
ZONDEREINDE
ZONDEREINDE
KOPJE ALLEEN
KAALVLAKTE
D
0.0 km
2.5 km
5.0 km
7.5 km
12.5 km
1500 m
1250 m
1000 m
D
D1
2.5 km
5.0 km
7.5 km
10.0 km
12.5 km
15.98 km

E

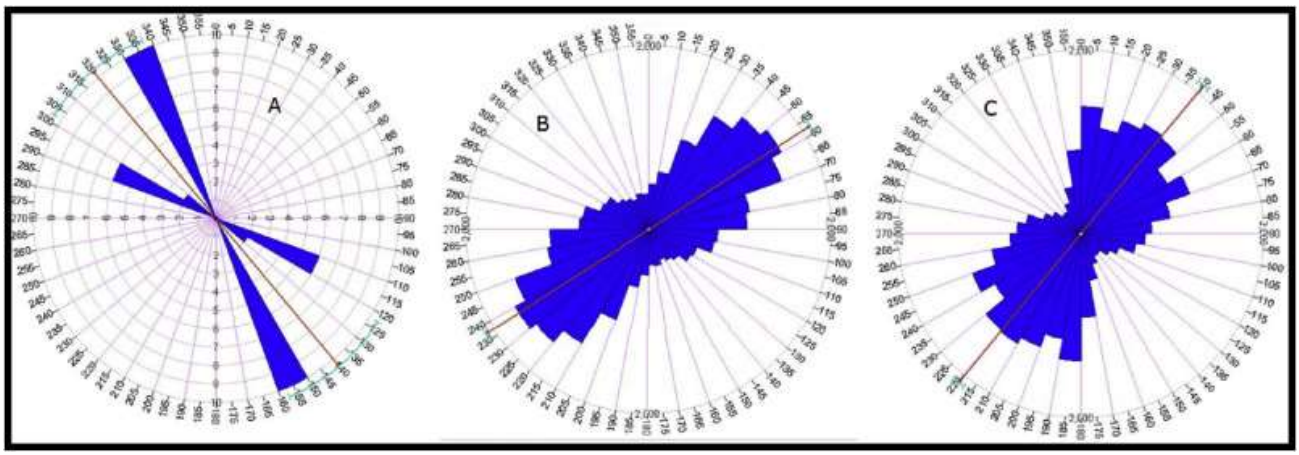

Fig. 2.
A: The Upper Zone top interval structure contour map with draped geologic outline (orange lines) of Amandelbult section of the Northwestern Bushveld Complex. The dots represent some of the borehole points.
B: Structure contour map for the top of the Main Zone interval draped with geologic outline (solid orange lines) and inferred faults represented as broken lines extracted from interval isopach maps of Amandelbult section of the Northwestern Bushveld Complex. The upthrown sides are indicated as U and downthrown sides as D along the major fault zones in the area.
C: The Main Zone base interval structure contour map of Amandelbult section showing a profile along the Roodedam graben (on Middellagte farm), the geological contact outlines and some of the inferred fault planes (blue dash lines). Note the concave nature (depression/negative structure) on profile B-B1 and the convex (positive thickness) nature on profile A-A1 in Fig. 2D.
D: The Main Zone interval isopach map of Amandelbult section showing profile A-A1 along the Roodedam graben (on Middellagte farm), the geological contact outlines and some inferred fault planes. Profile D-D1 shows the thickness of the magma deposit in this area. This same area shows a trough/depression on Fig. 2C (Profile C-C1).
E: Rose diagrams showing the major structural trends for the Upper Zone (A), Main Zone (B) and Lower Zone (C) intervals in the Amandelbult section of the Western Bushveld Complex.

that were structurally negative e.g. the graben area and depressions, show positive thickness on the isopach map, indicating that the structure was already in place before the influx of the magma. A step-like, south dipping NE trending fault that extends horizontally over a distance of approximately 22 km, separating the northern part from the southern part (Figure 2C, and 2D) can be inferred at the centre of the Amandelbult section. The present-day deeper section with thicker magma occurrence is the southern part of the Amandelbult section where the Main Zone is better preserved with a thickness of over 2,200 m based on available borehole records, while

the downthrown section is the northern part with Main Zone thickness of less than 400 m (Figure 2D). Undulations around this area are aligned in a NE-SW direction. The northwestern part of the NE trending fault is downthrown on the Main Zone interval structure contour map (Figure 2B) but upthrown on the Main Zone interval isopach map (Figure 2C). Same applies to the southeastern part of the NE trending Fault.

Figure 2B shows the upthrown and downthrown sides of inferred faults around the Amandelbult area. The rose diagram shows the major orientation of structures on the Upper Zone, Main Zone and Lower Zone intervals (Figure 2E).

The Upper Zone, Main Zone and Lower Zone structural contour interval of the Northwestern Bushveld (Figures 3A, 3B and 3C) with the isopach maps (Figures 4A, 4B and 4C) show a prominent NW trend at the center (i.e. around the northern and southern gap areas).

Profile N-N1 across the Upper Zone interval isopach map (Figure 4A) indicates a central upthrow and a sharp downthrow to the northeast around the northern gap area. The northern gap area of the Main Zone interval isopach map is marked by closely spaced isolines, while the southern gap area shows sparse isolines to the west on the Main Zone isopach map (Figure 4B). The northern gap also coincides with closely spaced parallel contours on the Main Zone interval isopach map (Figure 4B). Centrally located L-shaped isolines on the Main Zone interval isopach map (Figure 4B) represent strike-slip faulting (cf., Paulson and Pescatore, 1979). However, the thickening trend is northeastward on the Main Zone interval isopach map and underlying stratigraphic units (Figure 4C). A fault plane indicated by closely spaced parallel isolines, which represent a rapid decrease in thickness, separates the Amandelbult section from the Union

A

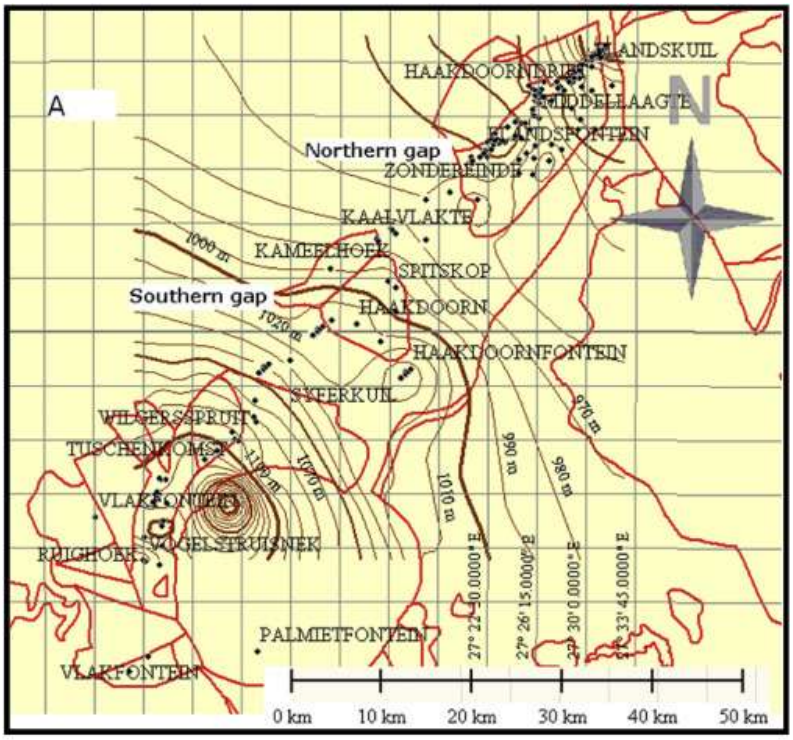
A
N
HAAKDOORNDRIFT
MIDDELLAAGTE
Northern gap
ZONDEREINDE
KAALVLAKTE
KAMEELHOEK
SPITSKOP
Southern gap
HAAKDOORN
HAAKDOORNFONTEIN
SYFERKUIL
WILGERSSPRUIT
TUSCHENKOMST
VLAKFONTEIN
VOGELSTRUISNEK
RUIGHOEK
PALMIETFONTEIN
VLAKFONTEIN
1000 m
1020 m
1070 m
1010 m
990 m
980 m
970 m
27° 22' 30.0000" E
27° 26' 15.0000" E
27° 30' 0.0000" E
27° 33' 45.0000" E
0 km
10 km
20 km
30 km
40 km
50 km

B

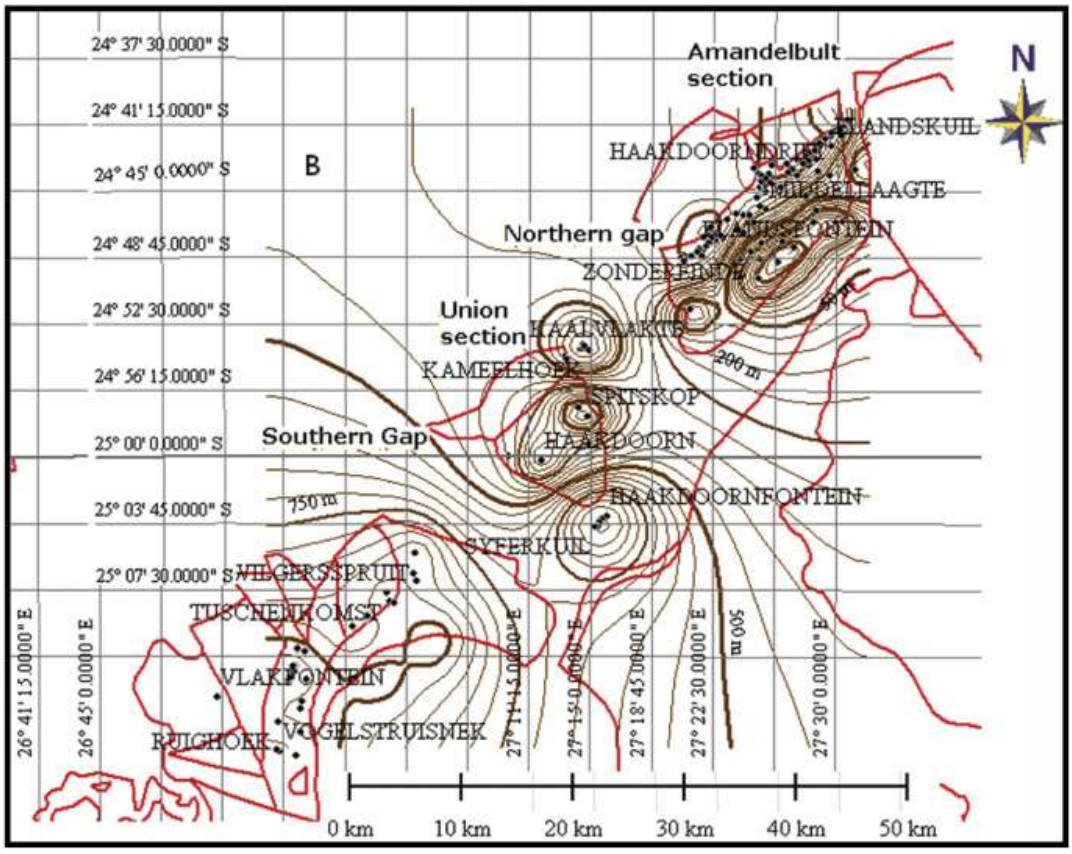
B
N
Amandelbult section
Union section
Northern gap
Southern Gap
HAAKDOORNDRIFT
MIDDELLAAGTE
ZONDEREINDE
KAALVLAKTE
KAMEELHOEK
SPITSKOP
HAAKDOORN
HAAKDOORNFONTEIN
SYFERKUIL
WILGERSSPRUIT
TUSCHENKOMST
VLAKFONTEIN
VOGELSTRUISNEK
RUIGHOEK
200 m
750 m
500 m
24° 37' 30.0000" S
24° 41' 15.0000" S
24° 45' 0.0000" S
24° 48' 45.0000" S
24° 52' 30.0000" S
24° 56' 15.0000" S
25° 00' 0.0000" S
25° 03' 45.0000" S
25° 07' 30.0000" S
26° 41' 15.0000" E
26° 45' 0.0000" E
27° 11' 15.0000" E
27° 15' 0.0000" E
27° 18' 45.0000" E
27° 22' 30.0000" E
27° 30' 0.0000" E
0 km
10 km
20 km
30 km
40 km
50 km

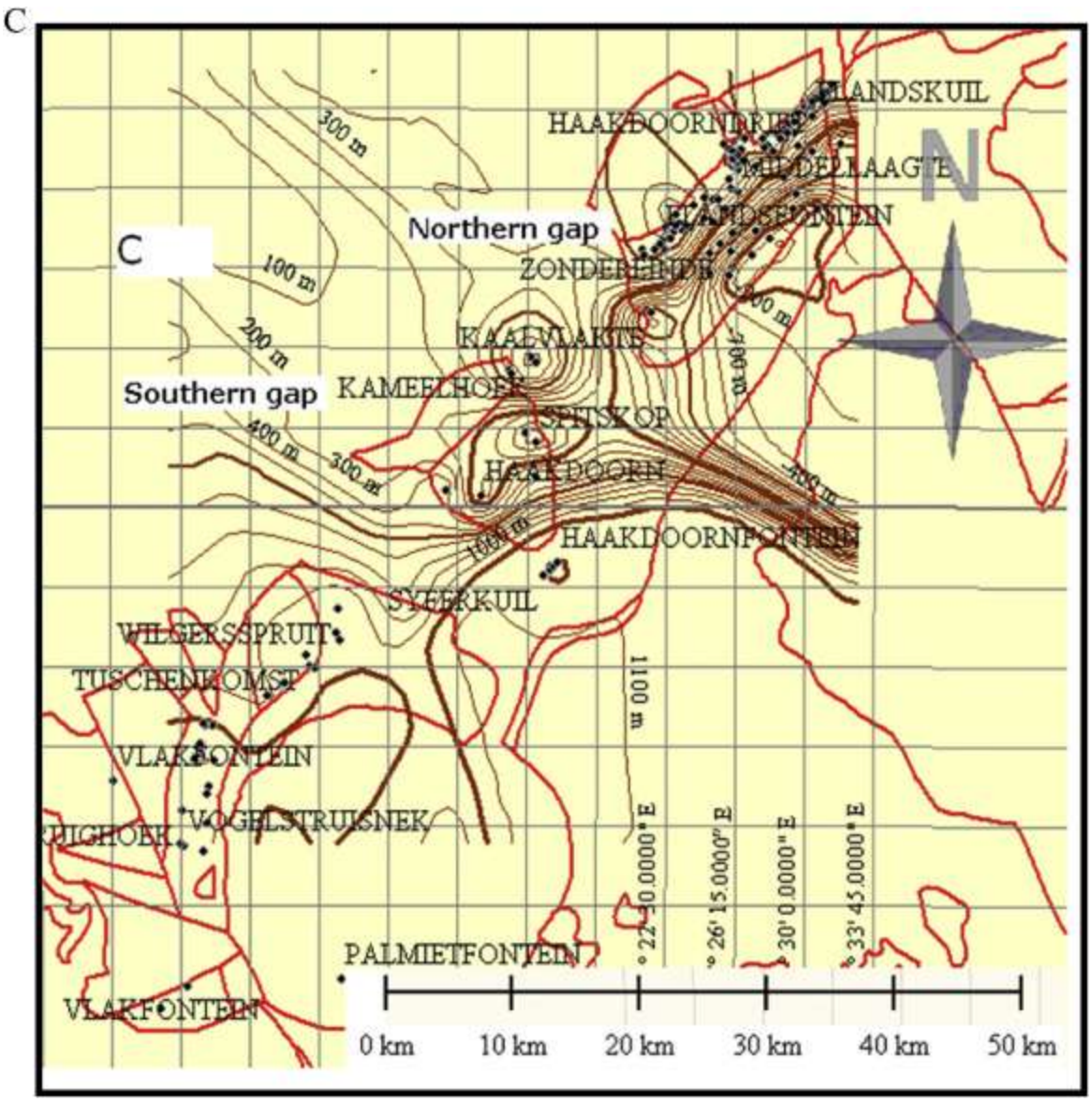

Fig. 3.
A: Structural map for the top surface of the Upper Zone interval in the Northwestern Bushveld Complex.
B: Interval structural map of the Main Zone base in the Northwestern Bushveld Complex.
C: Structural maps of the Lower Zone top interval in the Northwestern Bushveld Complex.

section of the Northwestern Bushveld Complex (Figure 4D). NW trending faults can be inferred at the central part of the Northwestern Bushveld Complex (Figures 4A and 4D). Rose diagrams show prominent NW-SE, NNE and NE-SW trends for the Northwestern Bushveld structures (Figure 4E).

A

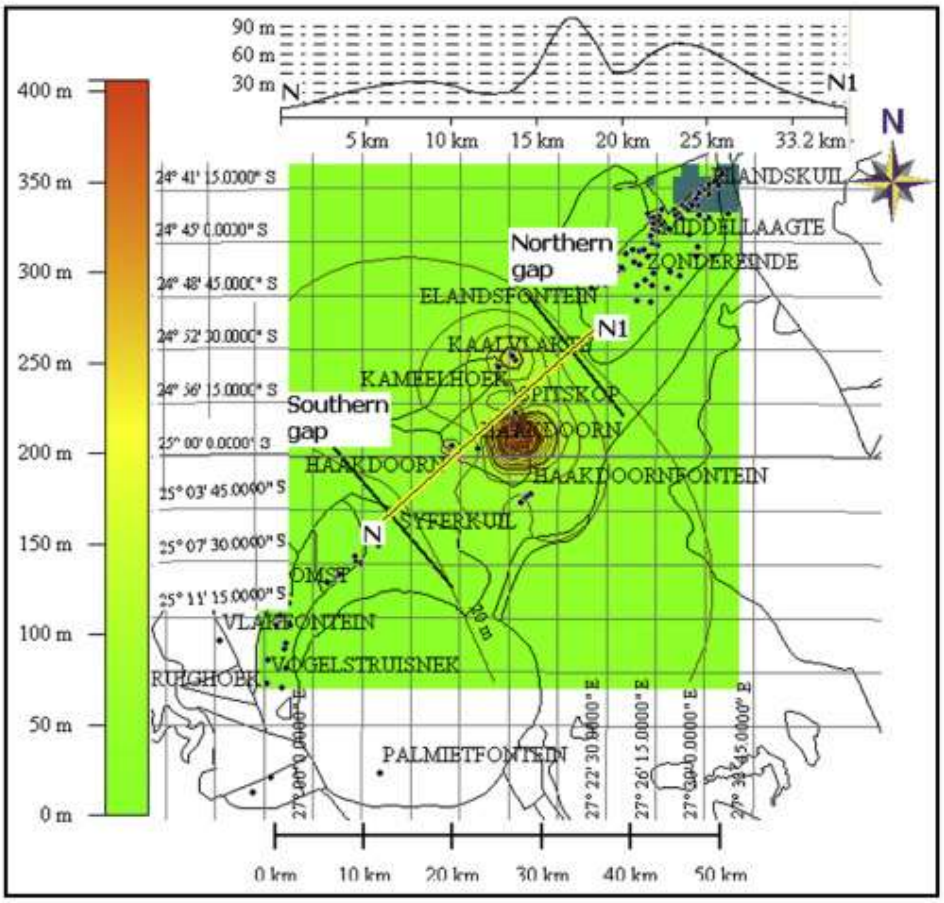
90 m
60 m
30 m
N
N1
5 km
10 km
15 km
20 km
25 km
33.2 km
400 m
350 m
300 m
250 m
200 m
150 m
100 m
50 m
0 m
N
Northern gap
Southern gap
ELANDSKUIL
MIDDELLAAGTE
ZONDEREINDE
ELANDSFONTEIN
KAALVLAKTE
KAMEELHOEK
PITSKOP
HAAKDOORN
HAAKDOORNFONTEIN
SYFERKUIL
OMSP
VLAKFONTEIN
VOGELSTRUISNEK
RUIGHOEK
PALMIETFONTEIN
0 km
10 km
20 km
30 km
40 km
50 km

B

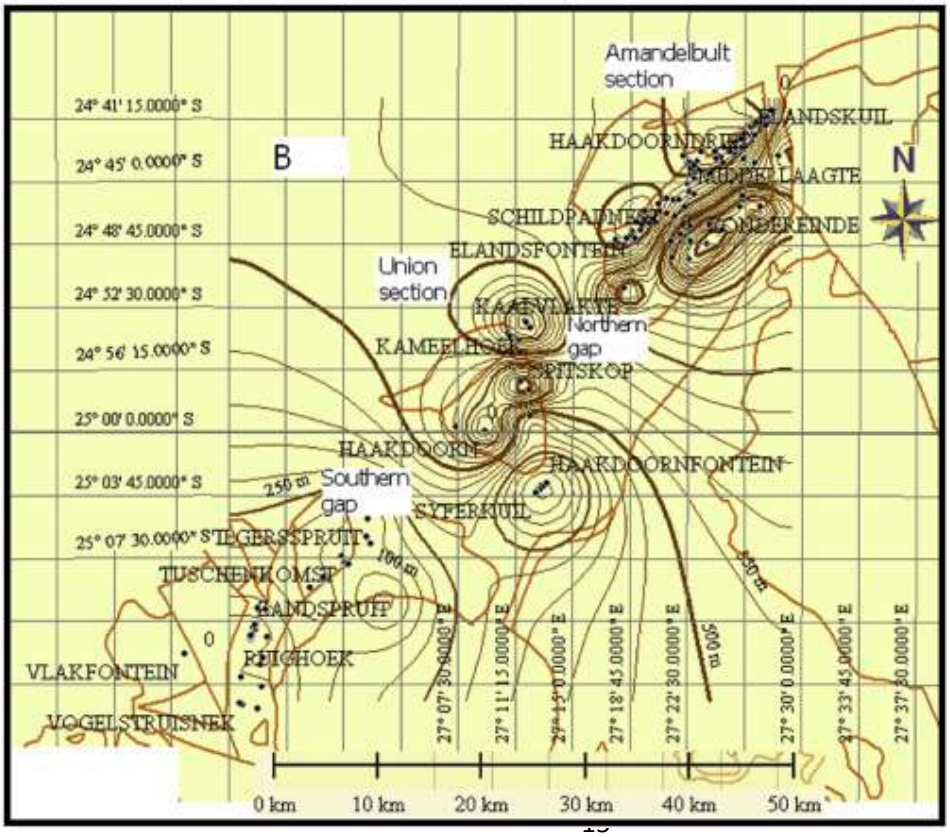
Amandelbult section
B
Union section
Northern gap
Southern gap
ELANDSKUIL
HAAKDOORNDRIF
MIDDELLAAGTE
SCHILDPADNEST
ZONDEREINDE
ELANDSFONTEIN
KAALVLAKTE
KAMEELHOEK
PITSKOP
HAAKDOORN
HAAKDOORNFONTEIN
SYFERKUIL
TEGERSPRUIT
TUSCHENKOMSP
BANDSPRUIT
RUIGHOEK
VLAKFONTEIN
VOGELSTRUISNEK
N
0 km
10 km
20 km
30 km
40 km
50 km

C

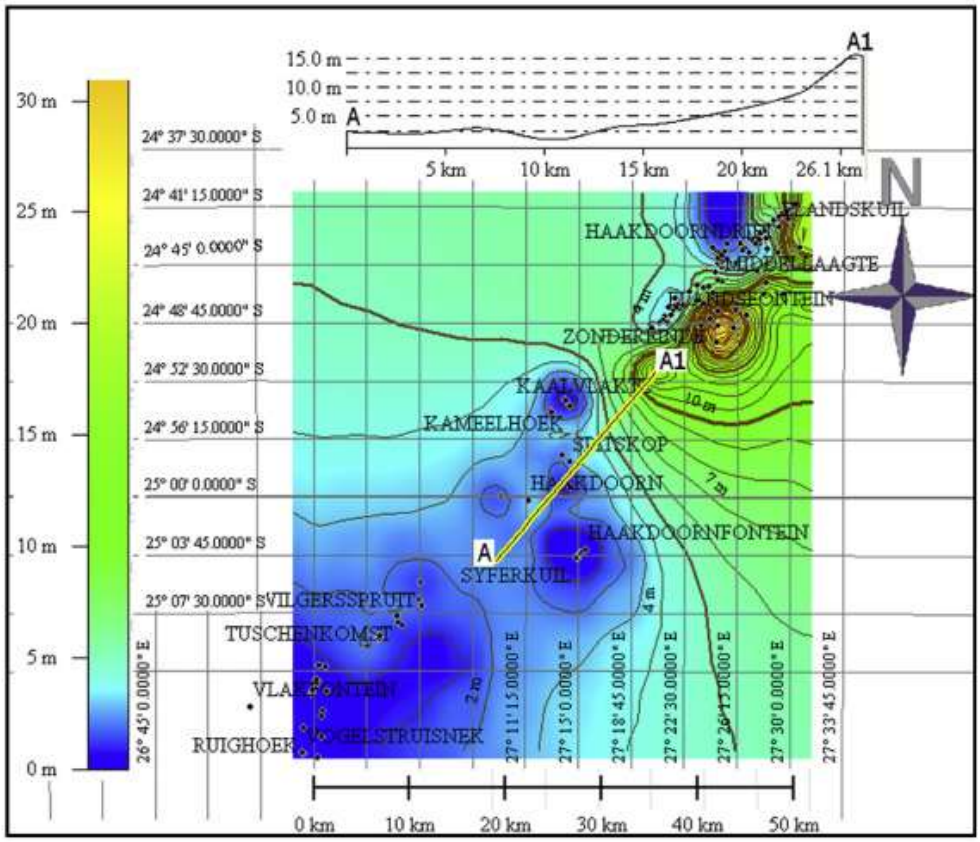
A1
A
15.0 m
10.0 m
5.0 m
5 km
10 km
15 km
20 km
26.1 km
N
30 m
25 m
20 m
15 m
10 m
5 m
0 m
24° 37' 30.0000" S
24° 41' 15.0000" S
24° 45' 0.0000" S
24° 48' 45.0000" S
24° 52' 30.0000" S
24° 56' 15.0000" S
25° 00' 0.0000" S
25° 03' 45.0000" S
25° 07' 30.0000" S
26° 45' 0.0000" E
27° 11' 15.0000" E
27° 15' 0.0000" E
27° 18' 45.0000" E
27° 22' 30.0000" E
27° 26' 15.0000" E
27° 30' 0.0000" E
27° 33' 45.0000" E
0 km
10 km
20 km
30 km
40 km
50 km
HAAKDOORNKUIL
ZANDSKUIL
MIDDELLAAGTE
ZONDERKUIL
KAALVLAKTE
KAMEELHOEK
SPITSKOP
HAAKDOORN
HAAKDOORNFONTEIN
SYFERKUIL
VILGERSSPRUIT
TUSCHENKOMST
VLAKFONTEIN
RUIGHOEK
VOGELSTRUISNEK
4 m
7 m
10 m
2 m

D

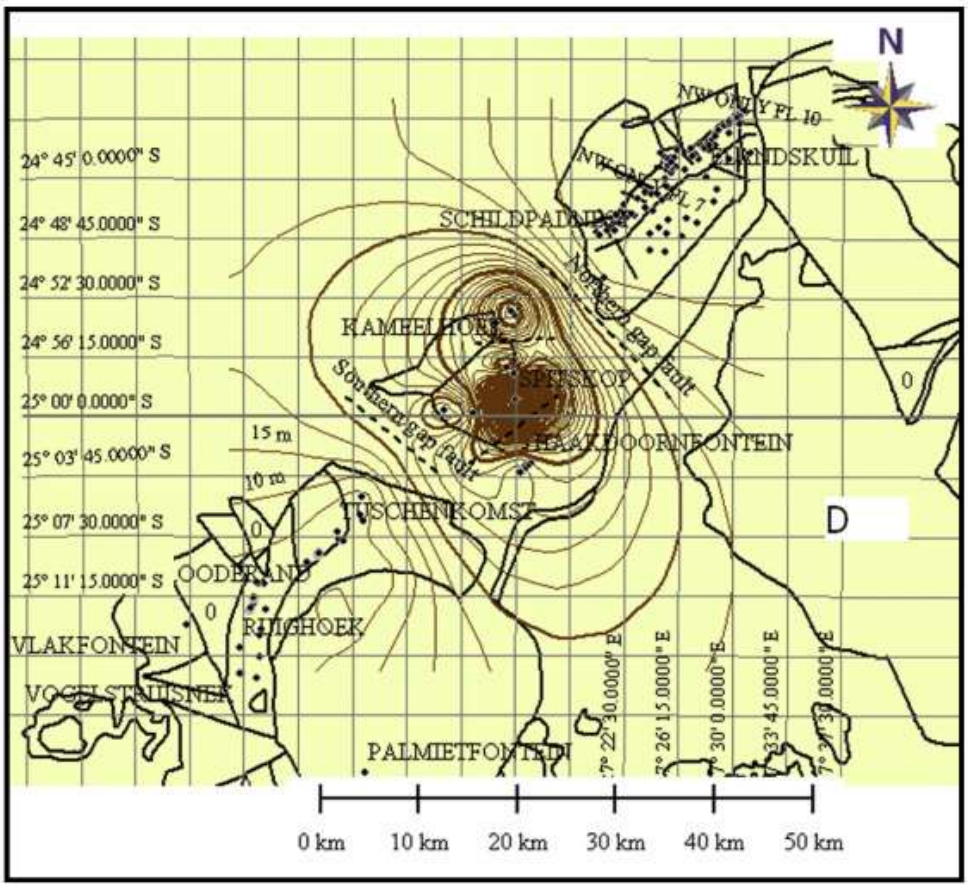
N
24° 45' 0.0000" S
24° 48' 45.0000" S
24° 52' 30.0000" S
24° 56' 15.0000" S
25° 00' 0.0000" S
25° 03' 45.0000" S
25° 07' 30.0000" S
25° 11' 15.0000" S
22' 30.0000" E
26' 15.0000" E
30' 0.0000" E
33' 45.0000" E
0 km
10 km
20 km
30 km
40 km
50 km
15 m
10 m
0
D
ZANDSKUIL
SCHILDPADFONTEIN
KAMEELHOEK
SPITSKOP
HAAKDOORNFONTEIN
TUSCHENKOMST
OODEBRANDS
RUIGHOEK
VLAKFONTEIN
VOGELSTRUISNEK
PALMIETFONTEIN
Northern gap fault
Southern gap fault

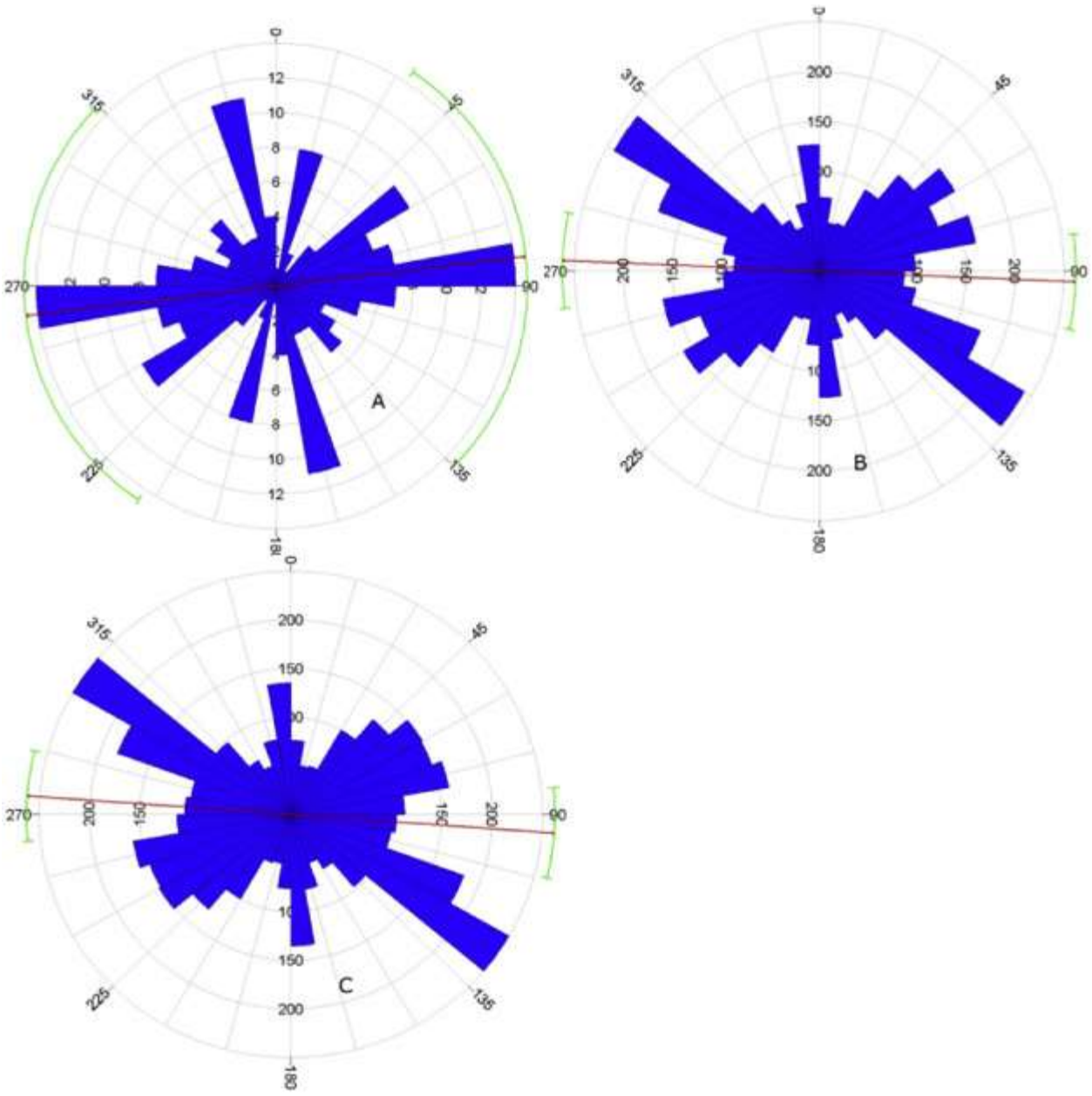

Fig. 4.
A: The Upper Zone interval isopach map showing profile N-N1 with shaper slope around the northern gap than the southern gap area of the Northwestern Bushveld Complex.
B: Main Zone interval isopach map in the Northwestern Bushveld Complex with NNW trending contours at the center. L-shaped contour lines between the Union section and the Southern gap signify strike-slip faulting.
C: Merensky Reef interval isopach map in the Northwestern Bushveld Complex with profile A-A1 indicating increase in thickness towards the NE.
D: Inferred faults draped on Upper Zone isopach map in the Northwestern Bushveld Complex.
E: A, B and C represent the rose diagram for the major structural trends on the Upper, Main, and Lower Zone intervals in the northwestern parts of Western Bushveld lobe respectively.

A

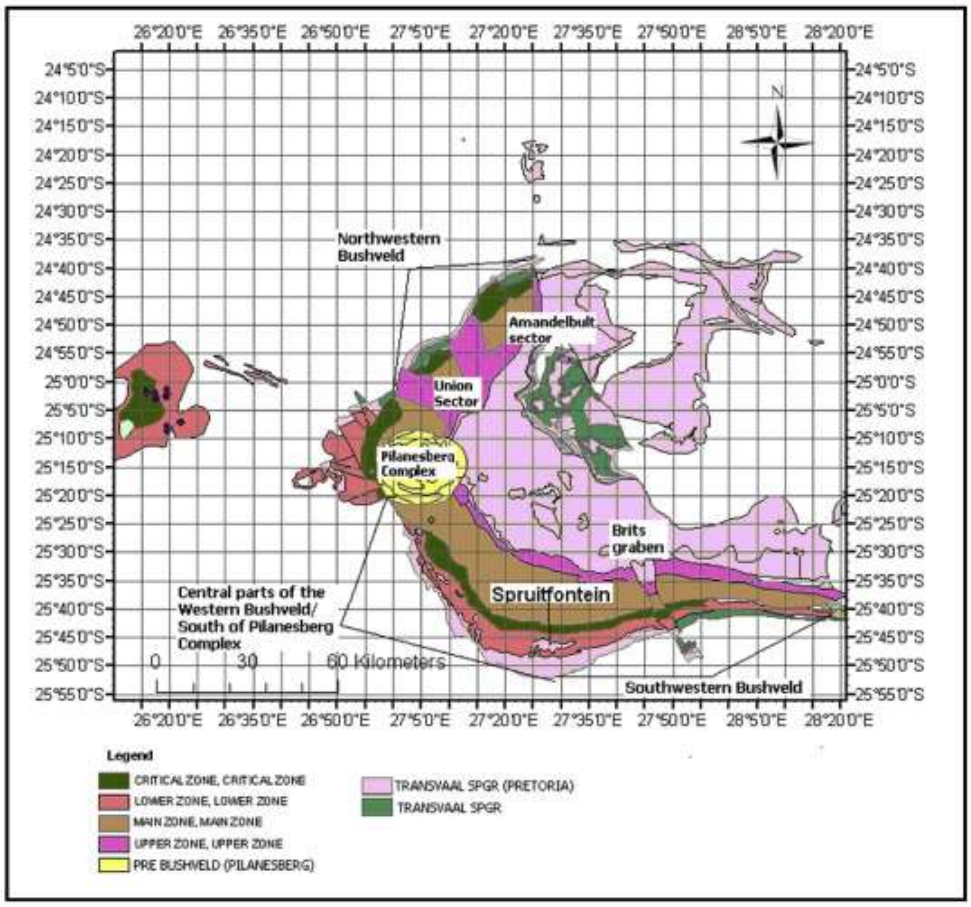
Northwestern Bushveld
Amandelbult sector
Union Section
Pilanesberg Complex
Brits graben
Spruitfontein
Central parts of the Western Bushveld/ South of Pilanesberg Complex
Southwestern Bushveld
0 30 60 Kilometers
Legend
CRITICAL ZONE, CRITICAL ZONE
LOWER ZONE, LOWER ZONE
MAIN ZONE, MAIN ZONE
UPPER ZONE, UPPER ZONE
PRE BUSHVELD (PILANESBERG)
TRANSVAAL SPGR (PRETORIA)
TRANSVAAL SPGR

B

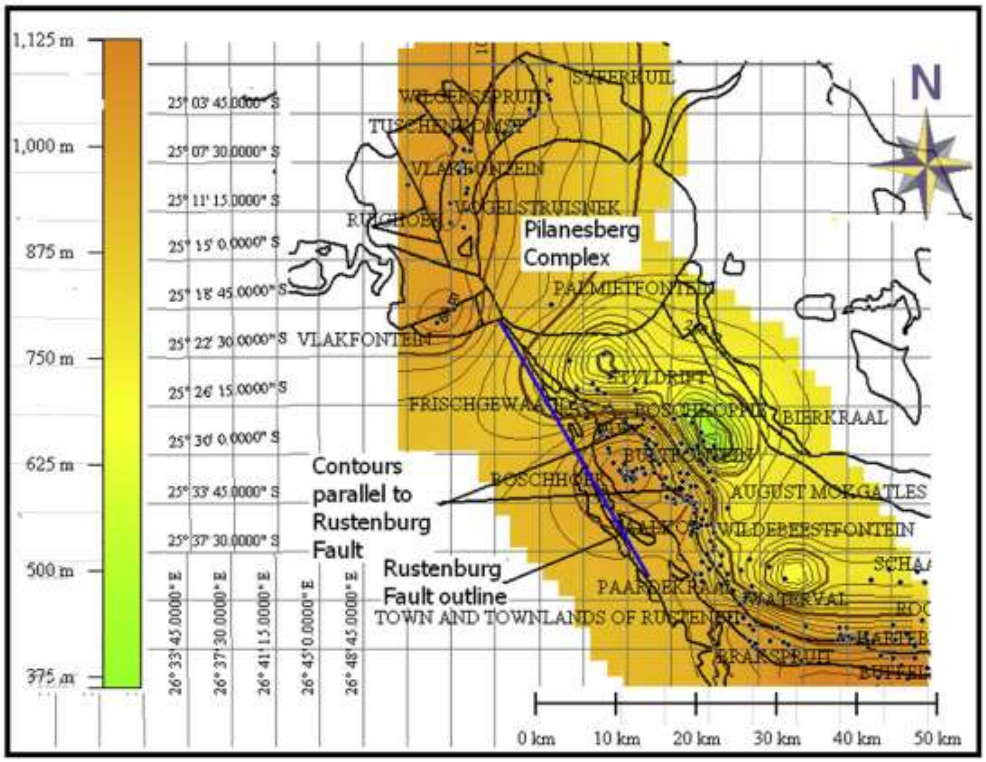
1,125 m
1,000 m
875 m
750 m
625 m
500 m
375 m
Pilanesberg Complex
Contours parallel to Rustenburg Fault
Rustenburg Fault outline
TOWN AND TOWNLANDS OF RUSTENBURG
0 km 10 km 20 km 30 km 40 km 50 km

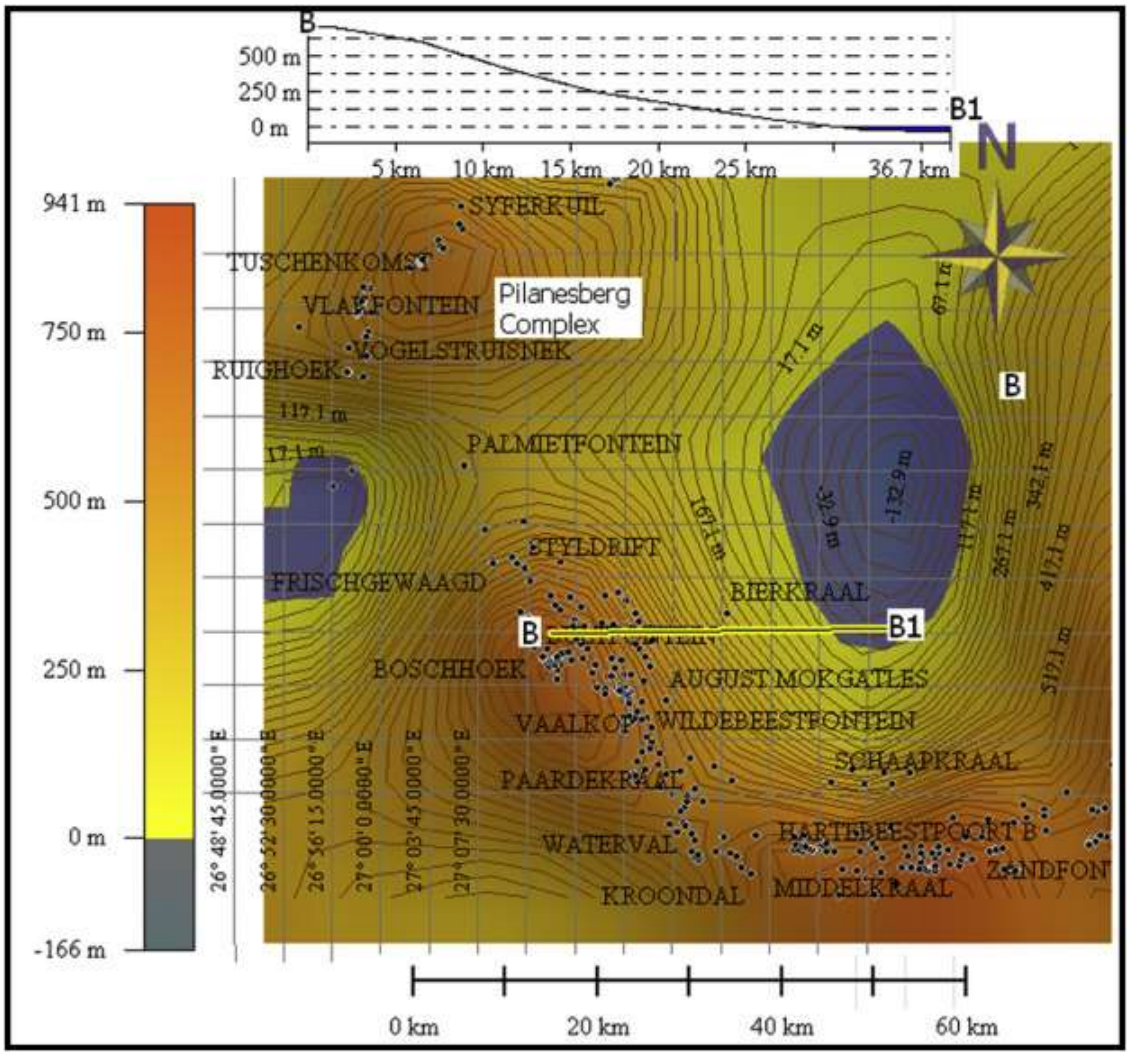

Fig. 5.
A: Geological map of the Western Bushveld Complex showing the parts of the BC to the north and south of the Pilanesberg Complex and the southwestern Bushveld referred to in text.
B: Main Zone interval isopach map of the southern parts of the Pilanesberg Complex area, showing fold axes trending approximately NW-SE trending isolines, parallel to the trend of the Rustenburg Fault.
C: Profile B-B1 drawn across the NNW-SSE trending isolines parallel to the trend of the Rustenburg Fault on the Lower Zone interval.

4.2 Structures around the Pilanesberg Complex of the Western Bushveld

The Pilanesberg Complex is located almost at the middle of the western lobe in the Bushveld Complex (5A). The southern part of the Pilanesberg Complex is marked by NW-SE trending isopach lines, which are parallel to the trend of the Rustenburg Fault (Figures 5B and 5C). The

northwestern part of the Rustenburg fault is made up of a NW-SE trending narrow structural high that dips towards the centre of the Western Bushveld Complex. Folds represented as closures aligned in a NW-SE direction in the Pilanesberg Complex area are indicated in Figure 5B. The Pilanesberg Complex area also slopes from the west to the east (i.e. dips towards the center of the Western Bushveld (Figure 5C)). An E-W trending structure contour pattern dominates the southern end of the Pilanesberg Complex (Figures 5B and 5C) especially on Kroondal farm, around the Spruitfontein upfold. This trend might represent dykes formed in the latter stage of a possibly Karoo event (Coomber, 2009). Structural trends observed on all the RLS stratigraphic intervals in this area include WNW, NW-SE, NNW, and NNE (Figure 6).

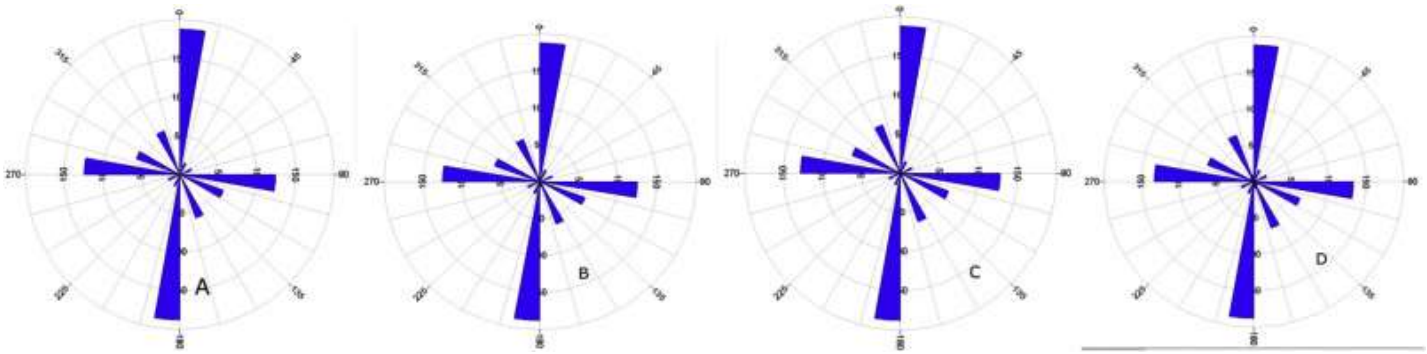

Fig. 6.
Rose diagrams of the major structural trends on Upper, Main Zone, Lower Zone and Marginal Zone intervals, respectively around the central part of Western Bushveld. Prominent structural trends include NNE, WNW, NNW and NE-SW.

4.3 Southwestern Bushveld Structures

The southwestern part of the Bushveld Complex (Figure 5A) is dominated by NNW-SSE trending faults around the town of Brits on both the interval structure (Figures 7, 8A and 8B) and isopach maps. Figure 7 shows the upthrown and downthrown sides of inferred faults extracted from structural contours and isopach maps of the area. The Main Zone interval structural map

reveals the presence of two graben-like structures at the western part of the Southwestern Bushveld around Schaapkraal farm (Figure 8A), to the north of the Spruitfontein fold. These two graben structures are bounded by faults, indicated by sharp slopes on the profile in Figure 8A. An anticlinal structure or structural high of over 250 m separates these two grabens. Another graben structure (Brits graben) occurs to the east around the Krokodildrift farm (Figure 7 and 8A). The center of this graben is flanked by two opposite dipping faults (Figures 7 and 8A): a NNW-SSE trending fault in the west and a NE-SW trending fault in the east. Most of the residual (small-scale) structures in the southwestern Bushveld occur along an ENE-WSW trend (Figure 8A).

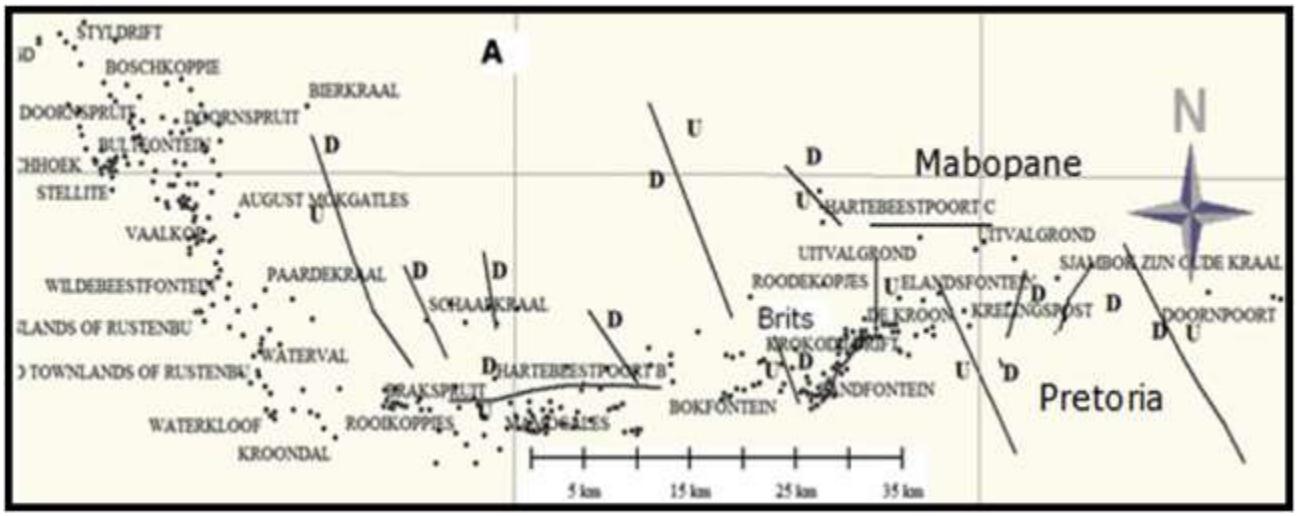

Fig. 7. Some of the inferred faults with the upthrown and downthrown sides in the Southwestern Bushveld.

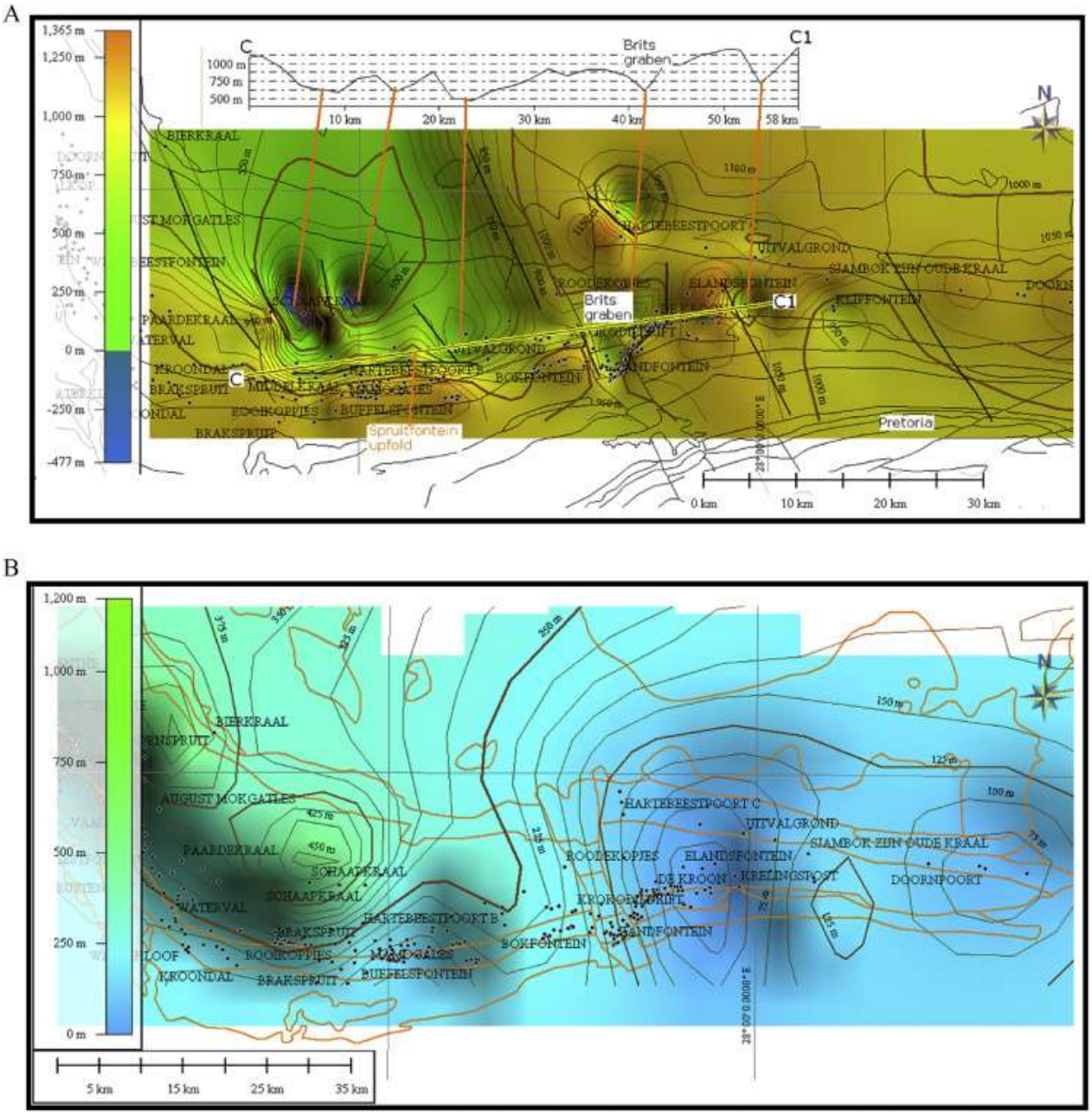

Fig. 8.
A: The Main Zone interval structural map showing the structural profile C-C′ with the location of the grabens in the Southwestern Bushveld.
B: Main Zone interval isopach map of southwestern part of Western Bushveld Complex.

A NNW-SSE trending fault can be inferred in the Hartebeestpoort C area and this coincides with the trend of the Brits Graben in the south (Figures 8A, and 8B). This fault shows a downthrow of

more than 1200 m on the Main Zone interval structural map. Northward thickening of the Upper Zone lithologies was observed on the isopach map in this area. More graben-like structures other than the Brits Graben occur in this sector (Figure 8A). The Brits faults are indicated on the RLS stratigraphic units. This suggests that the structure might represent an old structure that was reactivated during the emplacement of the RLS. There is thickening on the downthrown side and thinning on the upthrown side. Rose diagrams (Figure 9) highlighted the structural trends in this area.

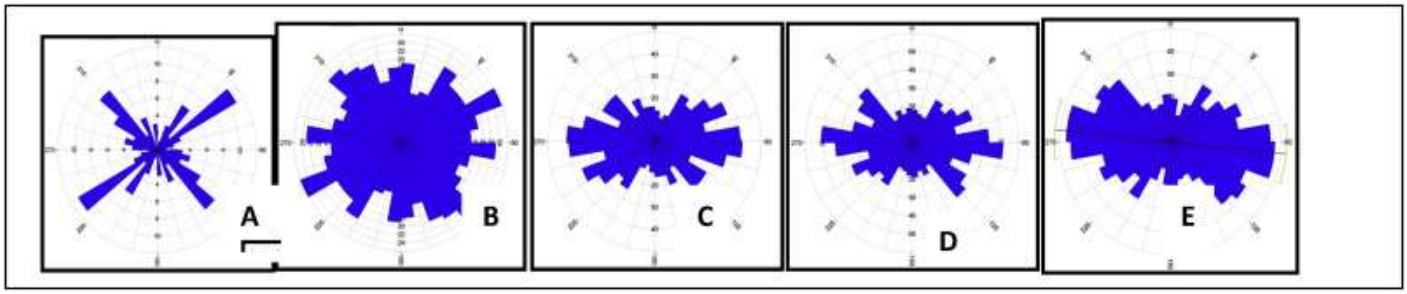

Fig. 9.
A to E represent rose diagram showing the interval structural trends at different stratigraphic intervals in the Southwestern Bushveld Complex indicating a change in trend with depth. A shows the structural trend on the Upper Zone top interval with prominent NW and NE orientations. B is the rose diagram of structures at the base of the Main Zone interval. C is the rose diagram showing the structural trend on the Merensky Reef interval, the prominent trend is E-W. D represents the UG2 interval structures with distinct E-W and NW trends. Trends on Lower Zone interval E) includes E-W and NW-SE orientations.

4.4 Structures similar to potholes

In the northern part of the Amandelbult section and south of the Pilanesberg Complex (Figure 5A), the large-scale pothole-structures have inverse shapes on the structure and isopach maps (see profiles in Figures 10 and 11). This suggests that these structures were already in place before the deposition of the magma and thus indicate structural control on the formation of potholes.

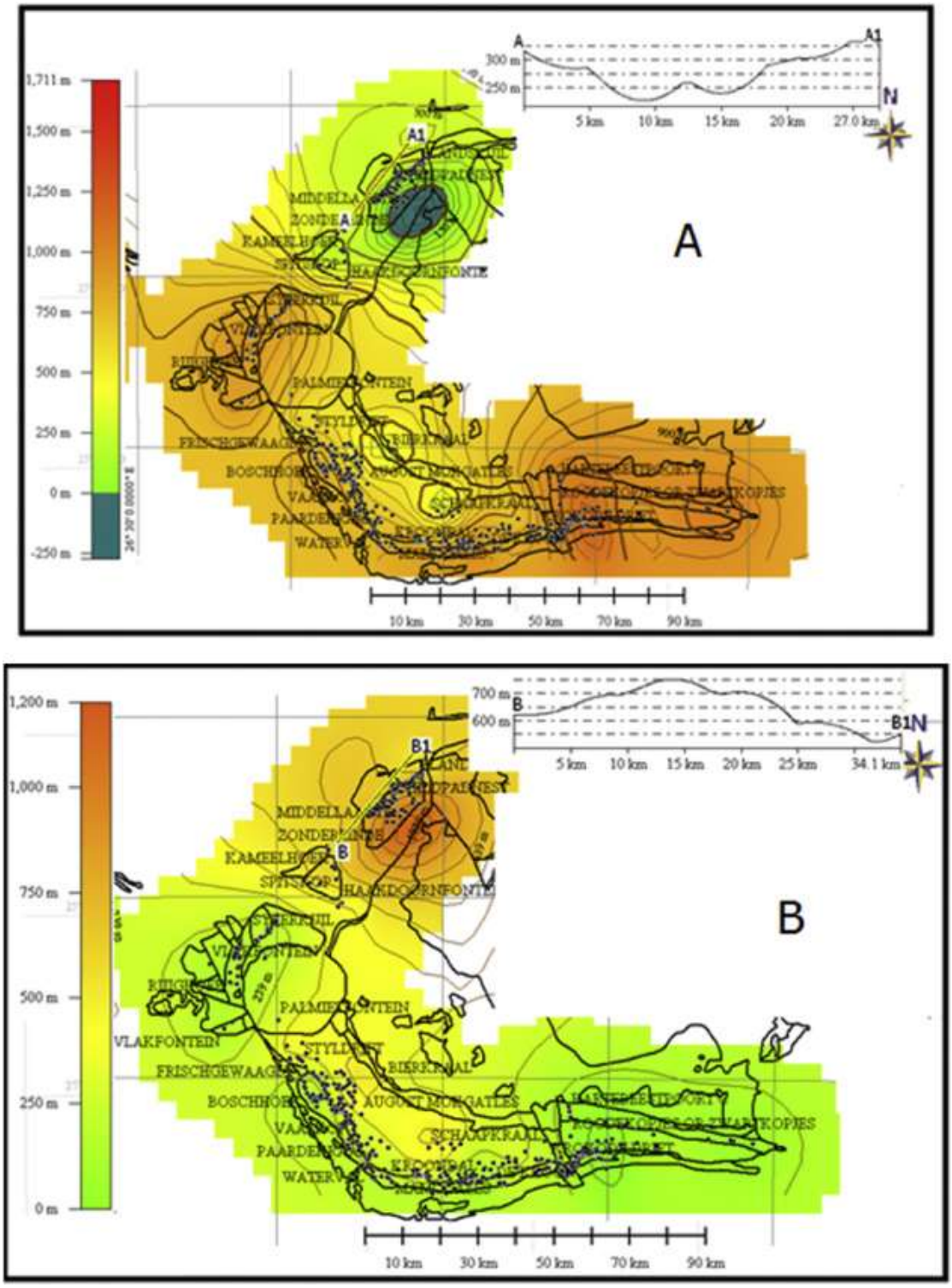

Fig. 10.
A: Profile A-A′ on Lower Zone interval structure contour map of Amandelbult section (A) and profile B-B′ on Lower Zone interval isopach map of Amandelbult section (B) of Western Bushveld showing the pothole-like structure feature on the structure and isopach maps of the area.

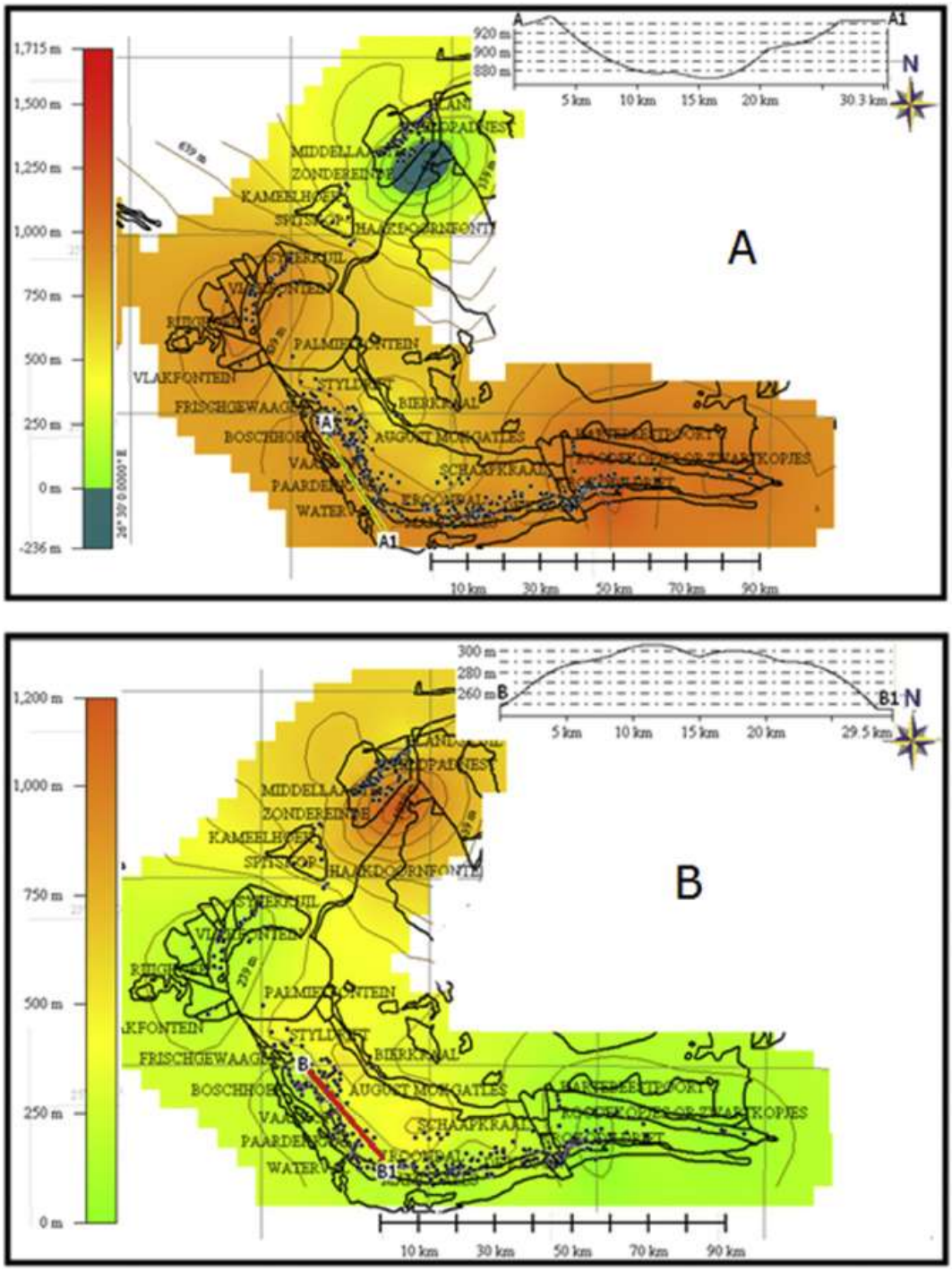

Fig. 11.
A: Profile A-A′ on Main Zone interval structure contour map (A) and profile B-B′ on Main Zone isopach map (B) of southern part of Pilanesberg Complex, Western Bushveld showing another pothole-like feature in the area. The inverse nature of the structure signifies that the structure was already in place before the magma infilling took place.

4.5 Eastern Bushveld Structures

The Eastern Bushveld Complex (Figure 12A) is marked by complex topographic undulation caused primarily by faulting, folding and doming (indicated by closures on the interval structure contours and isopach maps) in the floor rocks (Uken and Watkeys, 1997). Major faults such as the Wonderkop Fault, Stofpoort Fault, the Sekhukhune Fault Zone, Laersdrift Fault, and the Steelpoort Fault are all indicated to varying degrees on the interval isopach and structural contour maps (Figures 12B to 16).

Faults were inferred from closely spaced structure contours, variation in thickness across different stratigraphic horizons and sharp slope on profiles. The extreme western side of the Northeastern Bushveld Complex hosts a number of faults and folds as indicated on Figure 12B. One of these NNE-SSW striking faults is possibly the Stofpoort Fault. Another fault to the east runs almost parallel to the Stofpoort Fault. This fault separates the Fortdraai Anticline from a depression (marked as Eerste Regt or Phosiri grounds in Figures 12B and 12C). A profile across this fault shows a downthrow to the east (Figure 12C). The eastern boundary of the depression corresponds with the location of the Sekhukhune Fault. Around Katkloof dome, in the north another fault is inferred (Figures 12B, and 12C). This fault indicates a downthrow to the east.

The location of these identified faults coincides with known faults in the area and most of the faults trend approximately N-S. These faults are also downthrown to the east except for the Sekhukhune Fault which shows downthrow to the west (Figures 12B and 12C). The throw on each fault varies from 150 m to 2 km across the stratigraphic units. The Sekhukhune Fault trends almost N-S and has a maximum throw of about 2 km, east of the Fortdraai Anticline (Figures 12B and 12C).

A

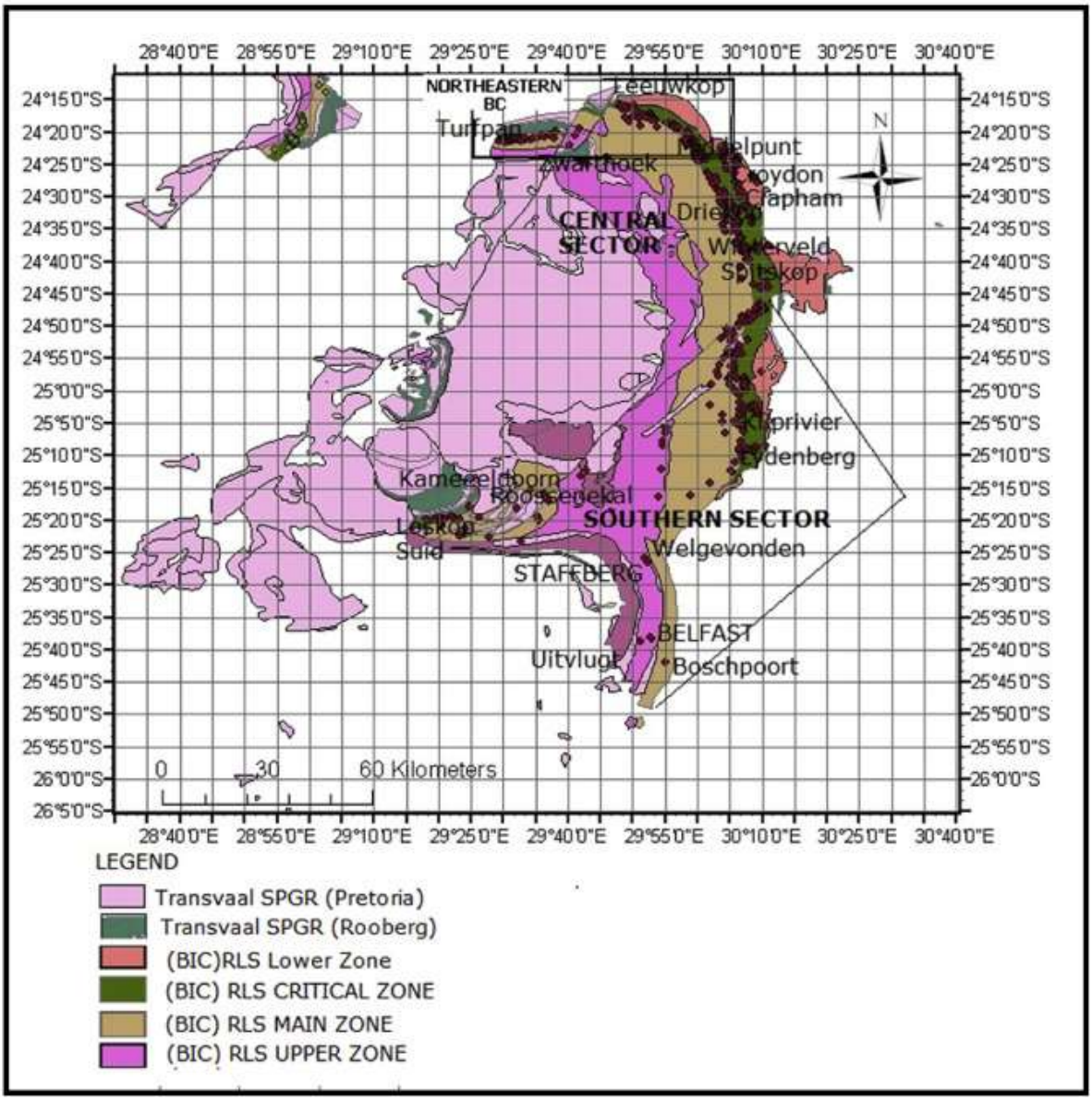

Fig. 12.
A: Geological map of Eastern Bushveld Complex showing the farm names and extent of sectors described in text.
B: Diagram showing Upper Zone structure contour interval with the geological contacts and some inferred fault locations draped over the Main Zone structural contour map of the Northeastern Bushveld.
C: The Main Zone structure contour map of the Northeastern Bushveld Complex showing profile B-B′ across Fortdraai anticline and adjacent depression at Eerste Regt and profile A-A′ across north-eastern part of Fortdraai anticline (along Katkloof dome and adjacent structure low area). Note the eastward dipping of faults in this section of the Eastern Bushveld.

B

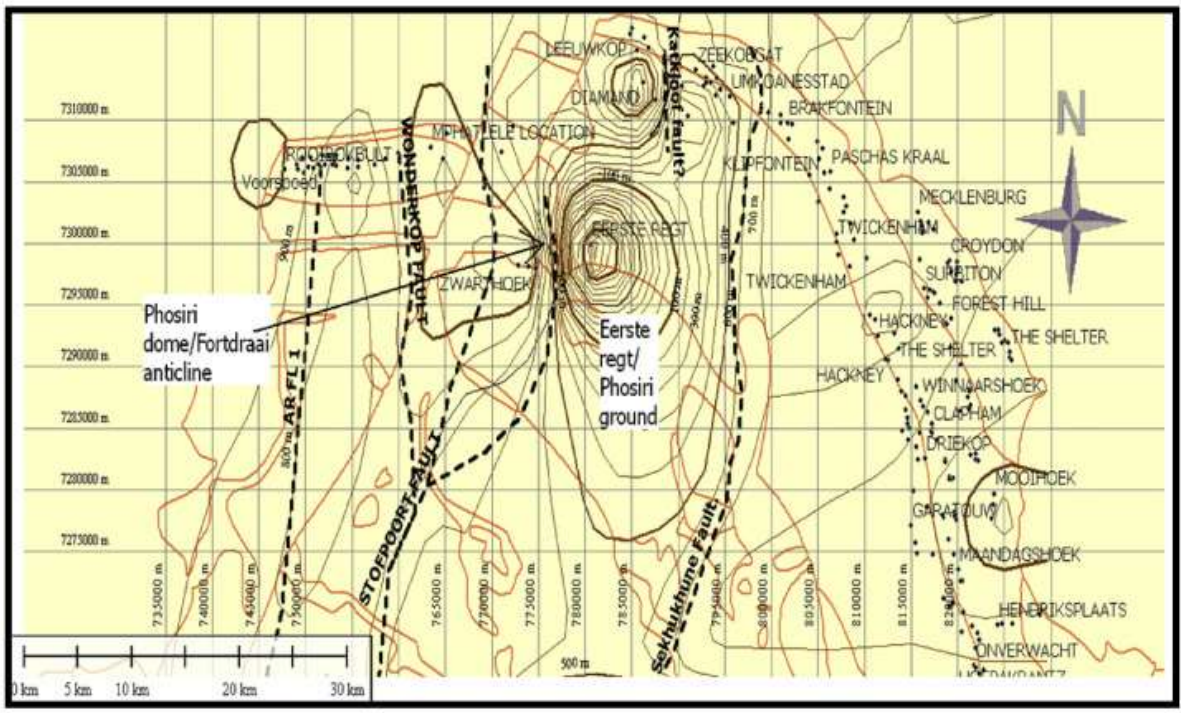
LEEUWKOP
ZEEKOEGAT
DIAMAND
UMKOANESSTAD
BRAKFONTEIN
MPHATELELE LOCATION
ROOIBOKBULT
Voorspoed
KLIPFONTEIN
PASCHAS KRAAL
MECKLENBURG
TWICKENHAM
CROYDON
SURBITON
FOREST HILL
HACKNEY
THE SHELTER
WINNAARSHOEK
CLAPHAM
DRIEKOP
MOOIPOEK
GARATOUW
MAANDAGSHOEK
HENRIKSPLAATS
ONVERWACHT
ERSTE REGT
ZWARTHOEK
Phosiri dome/Fortdraai anticline
Eerste regt/ Phosiri ground
WONDERKOP FAULT
STOEPOORT FAULT
Sekhukhune Fault
N
0 km 5 km 10 km 20 km 30 km

C

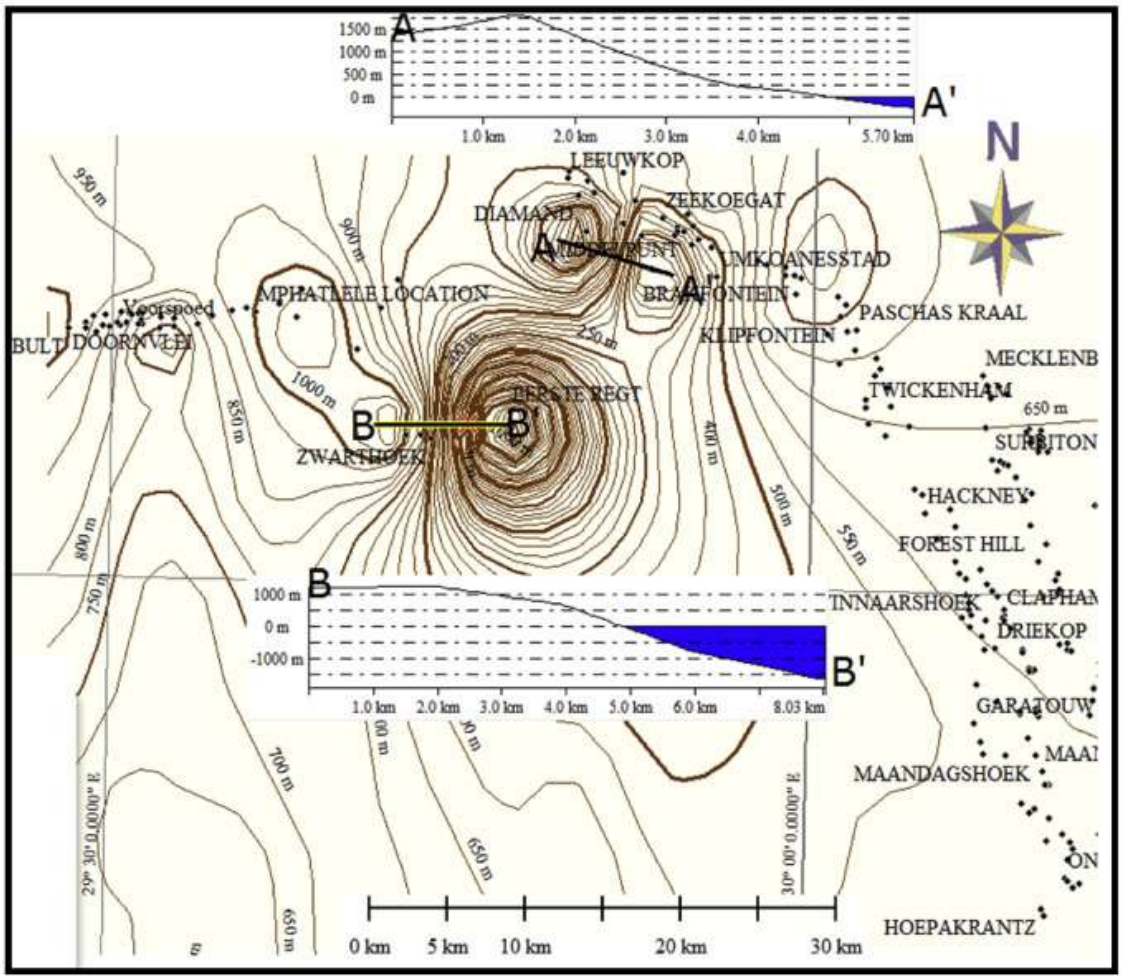
A
A'
1500 m
1000 m
500 m
0 m
1.0 km 2.0 km 3.0 km 4.0 km 5.70 km
B
B'
1000 m
0 m
-1000 m
1.0 km 2.0 km 3.0 km 4.0 km 5.0 km 6.0 km 8.03 km
LEEUWKOP
ZEEKOEGAT
DIAMAND
UMKOANESSTAD
BRAKFONTEIN
MPHATELELE LOCATION
Voorspoed
BULT
DOORNVLEI
PASCHAS KRAAL
KLIPFONTEIN
ERSTE REGT
ZWARTHOEK
TWICKENHAM
SURBITON
HACKNEY
FOREST HILL
INNAARSHOEK
DRIEKOP
GARATOUW
MAANDAGSHOEK
HOEPAKRANTZ
N
0 km 5 km 10 km 20 km 30 km

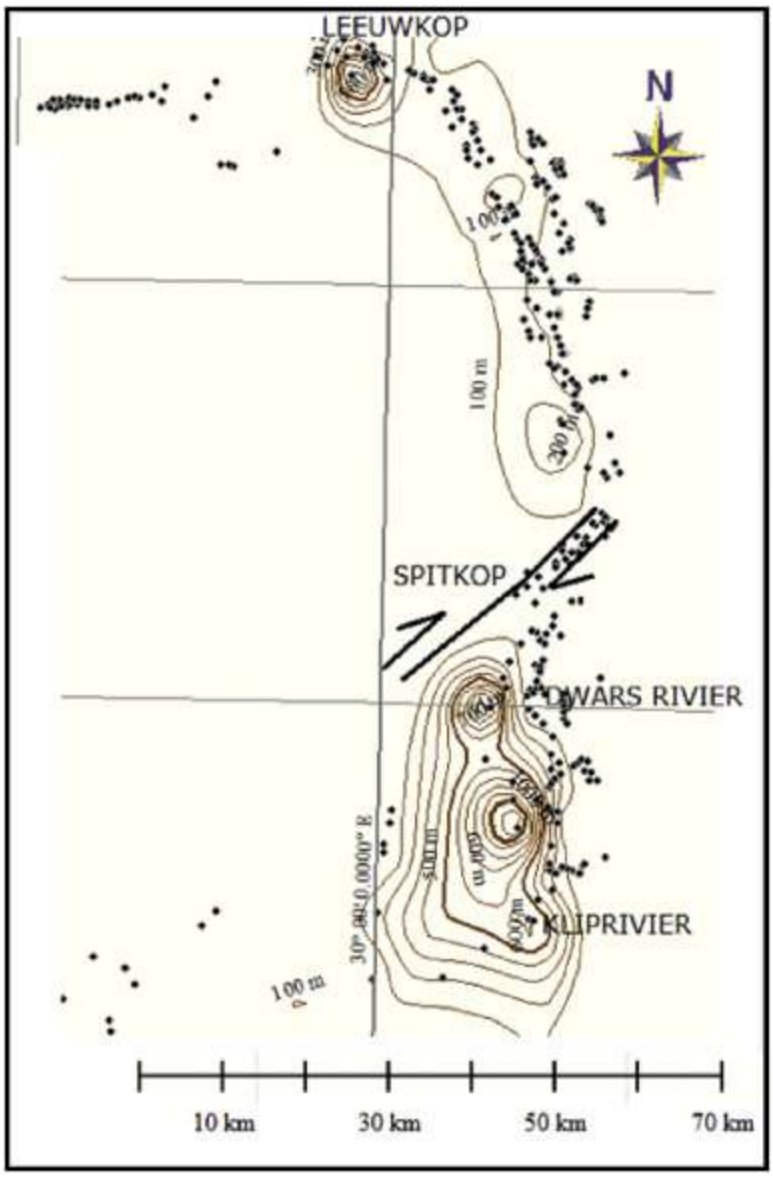

Fig. 13.
Main Zone isopach trend of the Eastern Bushveld showing Gap and left lateral movement between the Northern part and the Southern part, and the thickness variation of Main Zone rocks across the Steelpoort fault.

The Main Zone thickness variation across the Steelpoort Fault indicates lateral movement of the southern unit to the west and the northern portion to the east, with a gap around Kennedy's Vale (Figure 13). Two sets of faults can be inferred in the central part of the Eastern Bushveld section. The first one is a northern NNW-SSE trending fault that dips to the centre on Spitskop farm, and

the second one in the south strikes E to ENE (around Belvedere farm) and dips to the north thus creating a depression that coincides with the location of Kennedy's Vale (Figure 14).

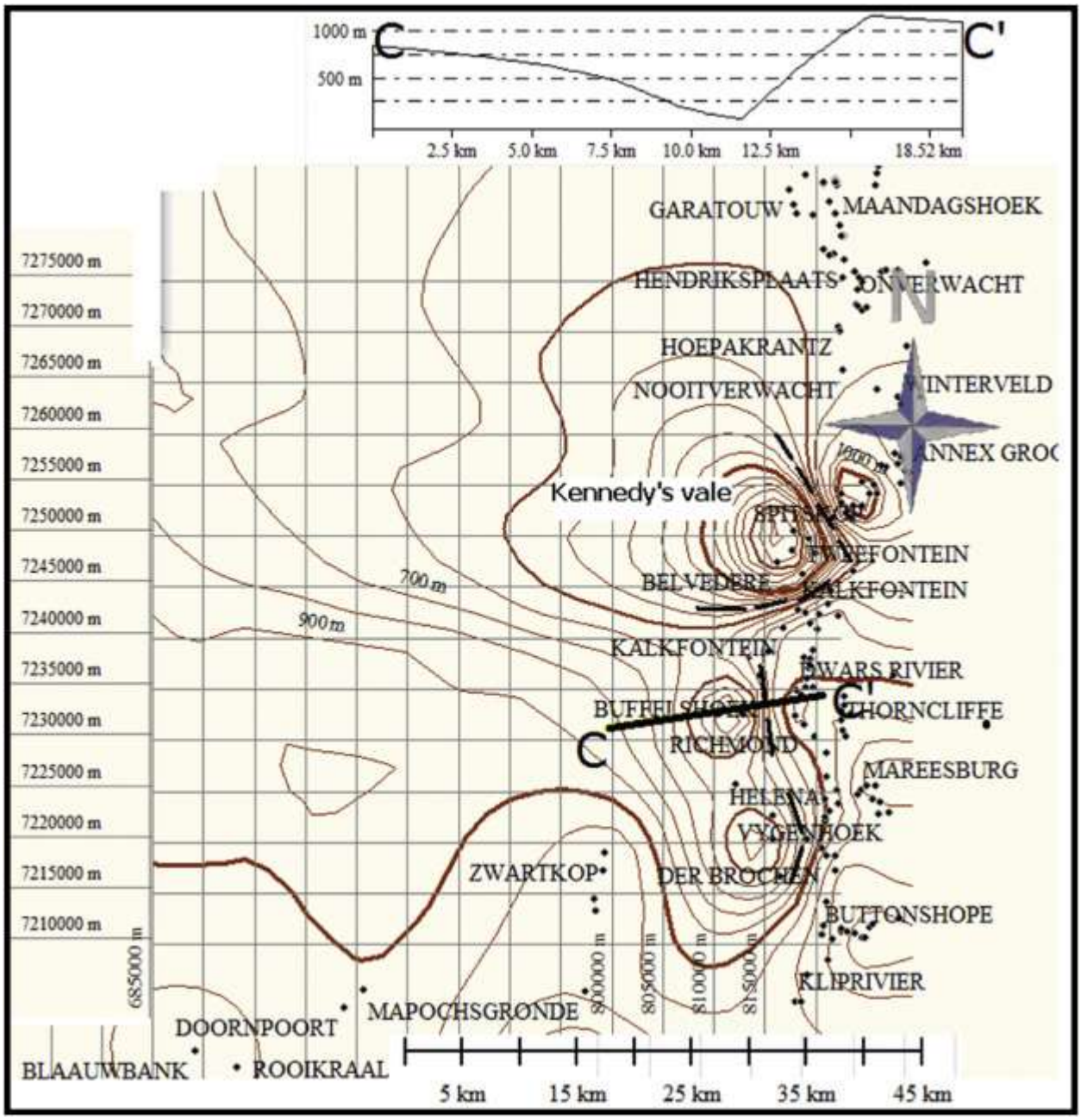

Fig. 14.
The Main Zone structure contour map showing the profile C-C′ across an inferred fault around Kalkfontein farm in the Southeastern Bushveld. Inferred fault and borehole locations are indicated with broken lines and black dots respectively.

A NNW trending fault is inferred around the southeastern portion of the Eastern Bushveld (Figure14); it extends from Kalkfontein farm southwards to the Klip Rivier valley area. Profile C-C' across this inferred fault shows a steep slope (Figure 14). The Main Zone rocks exhibit a westward thickening trend around the valley area while the same unit thins out eastwards. NW trending isolines on the Upper Zone interval structure contour map (Figure 15) represent the Laersdrift Fault.

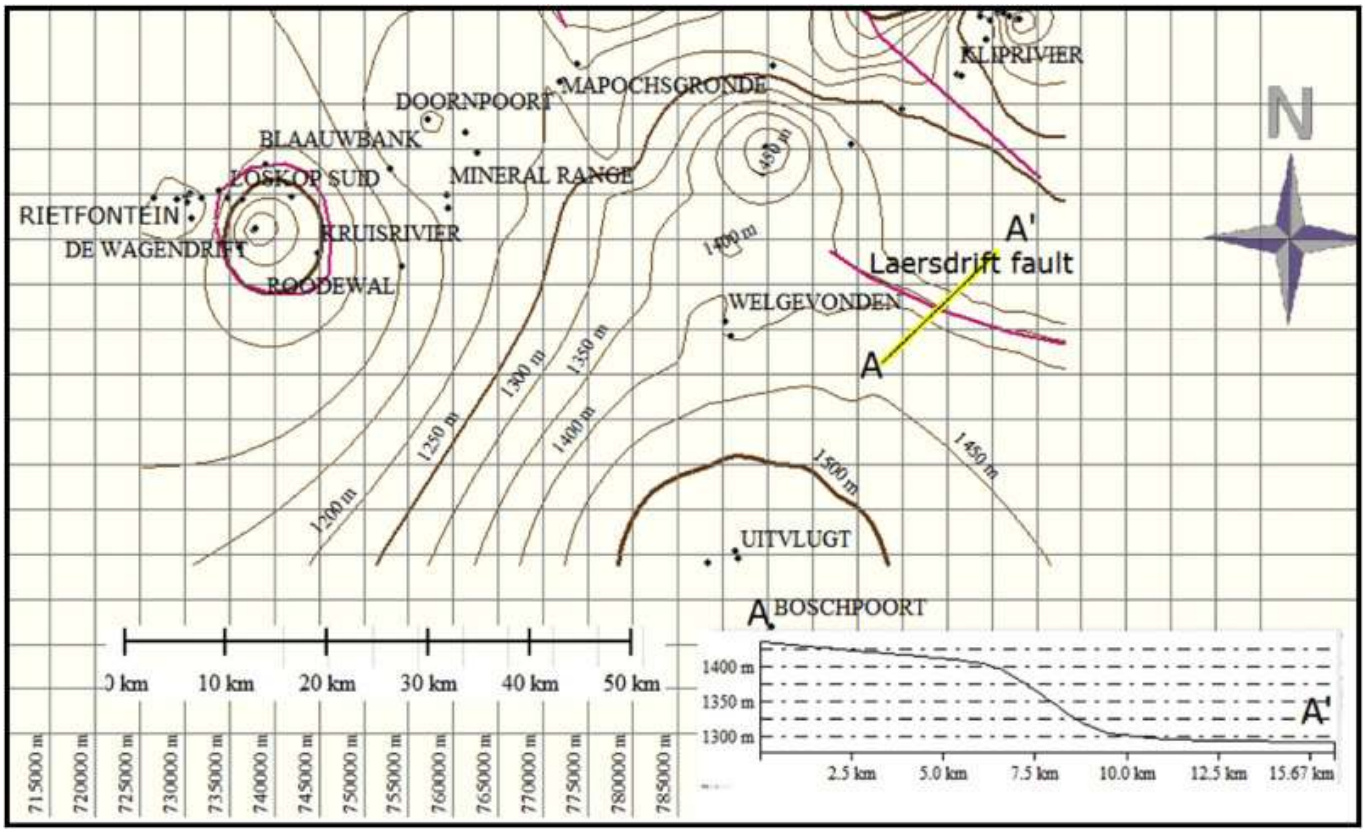

Fig. 15.
Upper Zone structure contour map with profile A-A′ showing the geometry and location of the Laersdrift fault in the southeastern part of the Eastern Bushveld Complex.

A

B

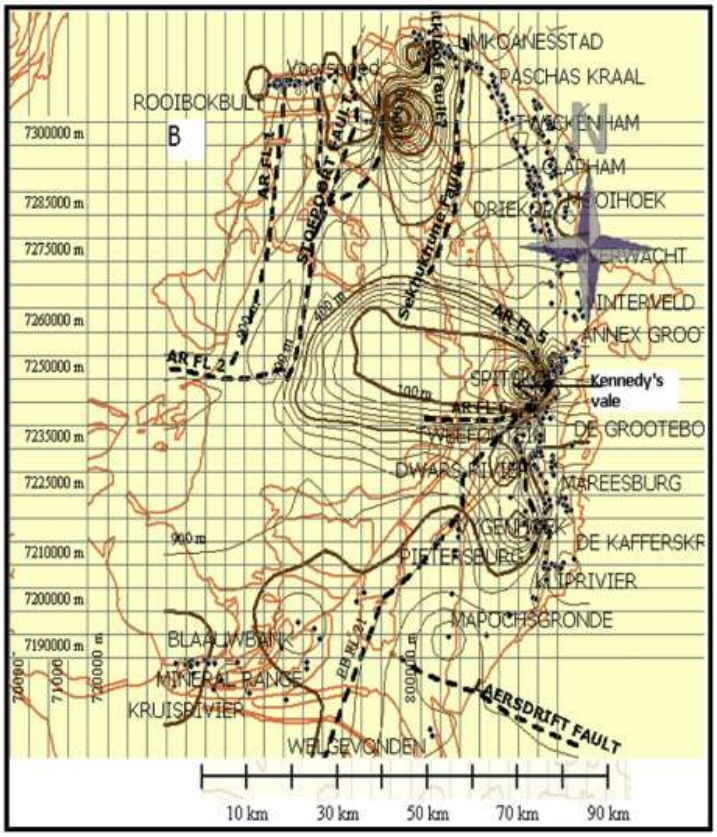

Fig. 16.
A: Diagram showing some of the inferred faults with the upthrown and downthrown sides in the Eastern Bushveld Complex.
B: Diagram showing Marginal Zone interval structure contours and some of the inferred faults in the Eastern Bushveld Complex.

Most of the faults in the northeastern Bushveld show downthrow to the east (Figures 16A and 16B) and trend approximately N-S while a few trend NNW and NE (Figure 17). However, the main trend in the Southeastern Bushveld is NNW-SSE (Figure 18).

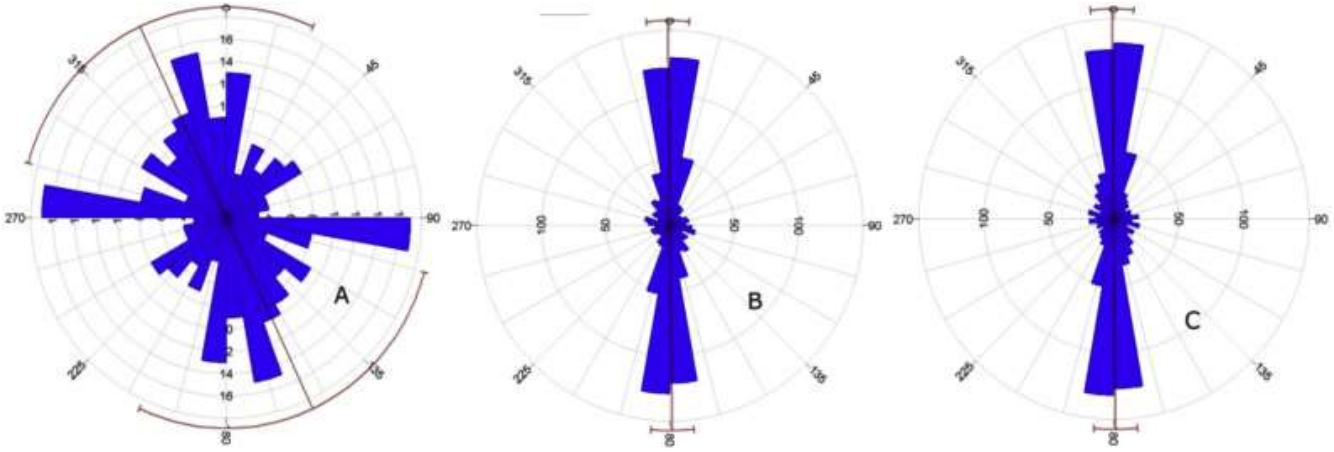

Fig. 17.
Structural trend rose diagrams for the Upper Zone interval (A) showing multiple peak orientation, Main Zone interval (B), and Archean rocks interval (C) of the Northeastern Bushveld Complex, showing prominent NNW, N-S and NNE trends.

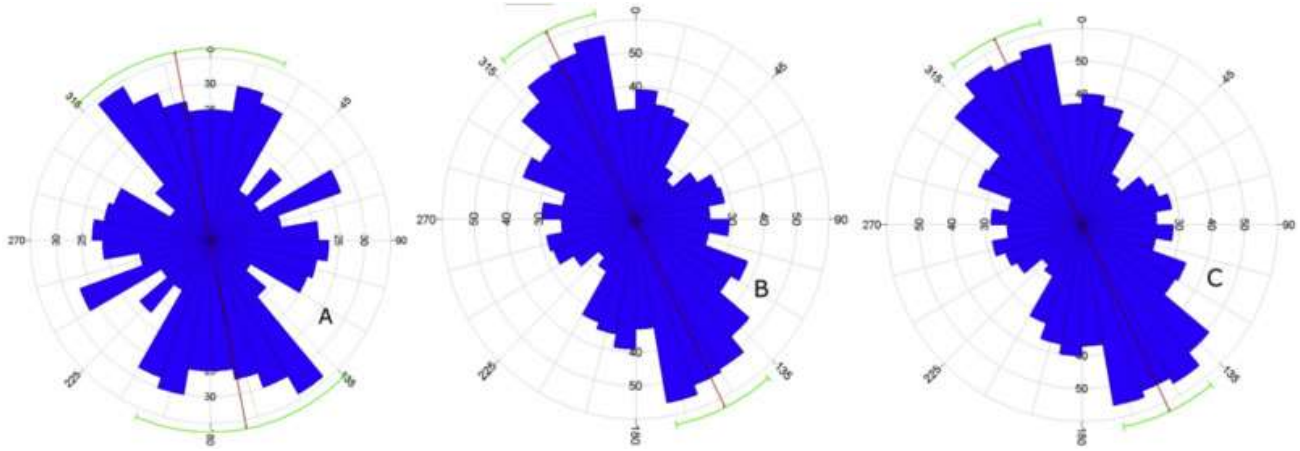

Fig. 18.
Main Zone (A), Lower Zone (B) and Archean rocks (C) interval rose diagram of the southeastern Bushveld Complex showing the major structural trends, oriented NNW-SSE.

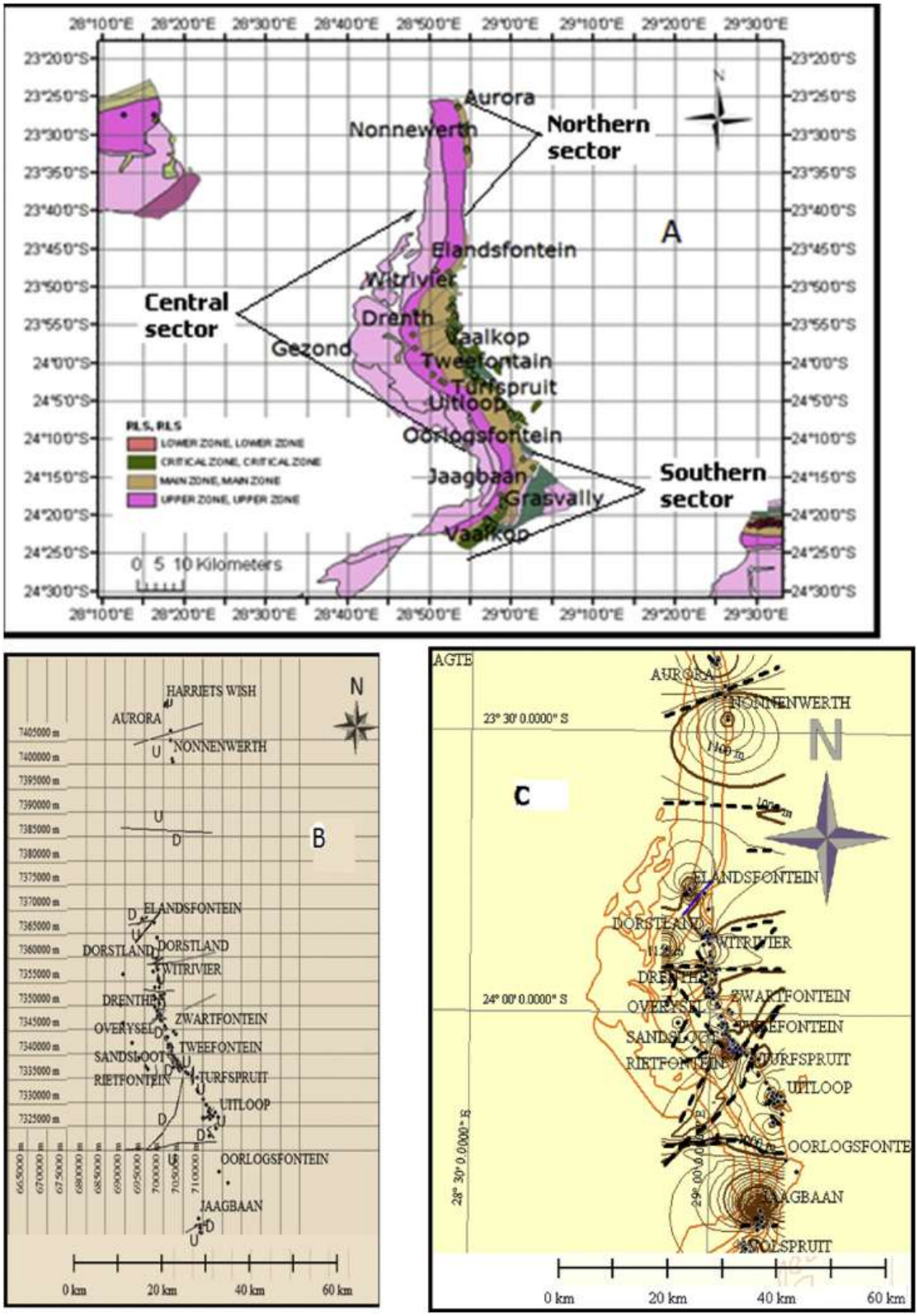

Fig. 19.
A shows the geological map with some of the locations mentioned in text. (B) Shows the inferred faults within the Northern Bushveld Complex with the upthrow and downthrow parts while, C shows the Marginal Zone structure contour map and inferred faults draped on the geological contacts.

4.6 Northern Bushveld Structures

The geologic map of the Northern Bushveld with the different sectors and farm names isshown in Figure 19A. Faults extracted from interval isopach and structure maps of the Northern Bushveld are compiled on Figures 19B and 19C, detailed descriptions of some of the faults are given below.

The far northern part of the Potgietersrus lobe or Northern Bushveld slopes sharply with a downthrow to the north, suggesting a NE trending fault (Figures 20A (ii) and 20A (iii)) between the farms Aurora and Nonnenwerth. Further northward toward the terminal edge of the lobe, a NW striking fault (profile E-E' on Figure 20B) is inferred between Harriet and Aurora farms. This fault has a downthrow of approximately 120 m to the SW.

Around Elandsfontein farm in the north-central part of the Northern Bushveld Complex (Figures 20A (i), (ii) and (iii)) a series of NE to ENE striking faults are inferred at different horizons. Further southeastwards, similar faults occur between Dorstland and Witrivier farms with downthrow to the north on Drenthe farm. On the southern part of the farm Overysel on Figure 20C two sets of faults can be inferred; the first set is E-W trending, while the second exhibits a NE-SW trend with downthrow to the south (Figure 20C). NNW-SSE striking faults with downthrow to the SW can be inferred at the separation point between Tweefontein Hill and the adjacent synclinal structure on Rietfontein farm i.e. south of Sandsloot farm (Figures 20A (ii) and 20A (iii)). This structure indicates a thick occurrence of RLS rocks in an area that was previously structurally negative (a depression) as indicated on the interval structure contour maps, suggesting that the structure was already in place before the emplacement of the RLS

rocks. The N-S trending faults inferred at the northwestern part of Turfspruit farm show upthrow to the east of Tweefontein farm (Figures 20A and 20B).

Uitloop farm in the southeastern extreme of the Northern Bushveld hosts a slightly curved NE striking fault, which appears on all the stratigraphic unit interval maps with the upthrown side to the southeast. A different E-W striking fault that separates the central part of the Complex from the southern part is inferred at the southern part of Uitloop farm. This fault is joined to another fault with a NE-SW trend, parallel to the Ysterberg-Planknek fault (represented with dash lines on Figure 20C).

The western part of the central northern Bushveld Complex displays an undulating and SE trending surface (profile C-C' in Figure 20B). A Northern Bushveld fence diagram in Figure 21 illustrates the internal structure and the geometric relationships of the RLS rocks. A wedge shaped feature at the southern end of the central sector (Figure 21 and profile B'-B in Figure 20B) probably represents the Kleinmeid Syncline discovered by Blaine (1973) and described by Van der Merwe (2008) as comprising noritic rocks occurring between the Grasvally structure and the Magaliesberg quartzite floor. The Kleinmeid Syncline terminates against the Grasvally Fault in the east. The floor rock exhibits ENE-WSW trending faults and downthrow to the NW (this suggests that the structure represents an old structure) around the Grasvally structure. Profile A-A' shows downthrow to the east and B'-B shows downthrow to the south. Rose diagrams in Figures 22 to 24 show the major structural trends in the three sectors of the Northern Bushveld.

A

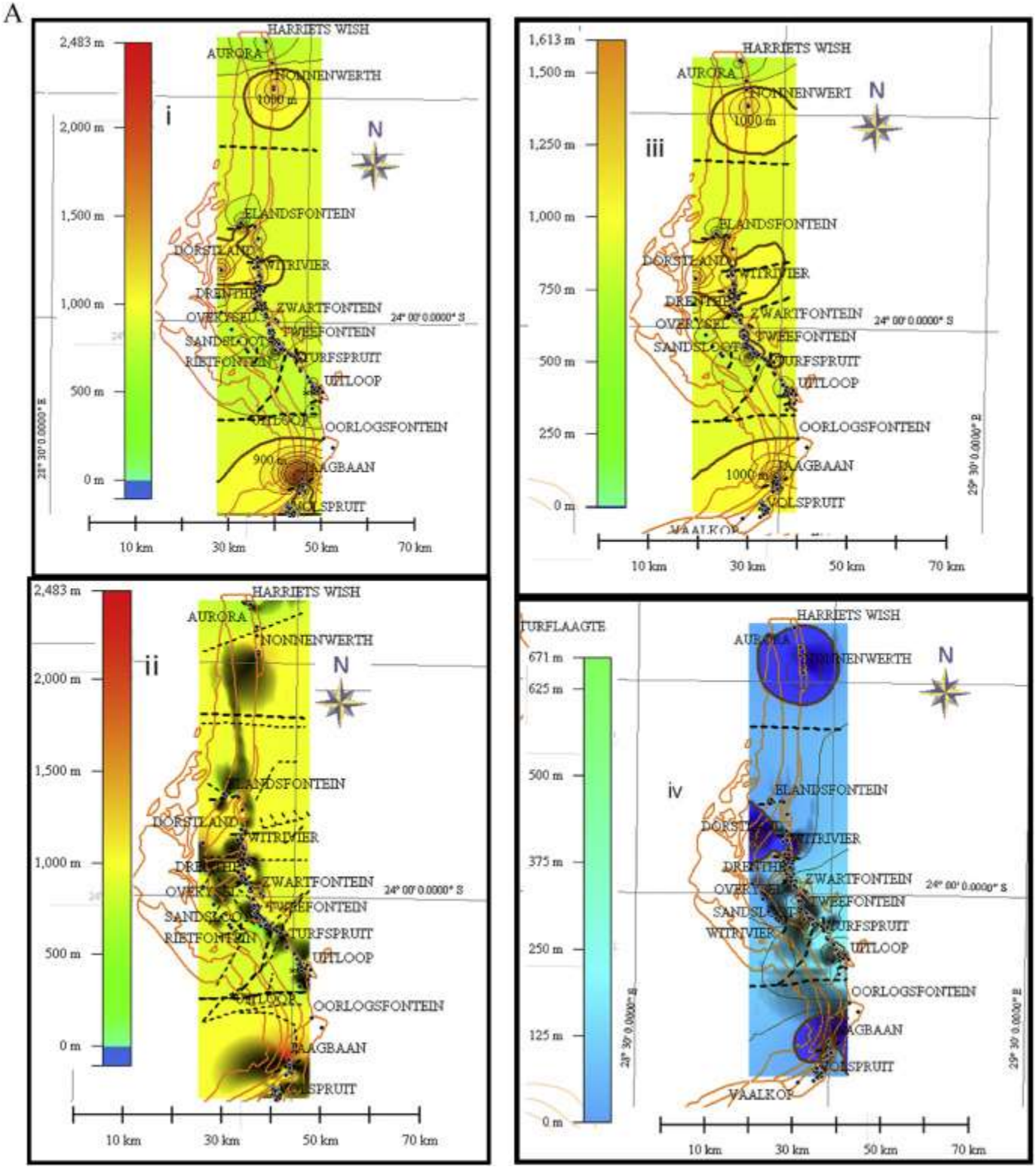
i
2,483 m
2,000 m
1,500 m
1,000 m
500 m
0 m
HARRIETS WISH
AURORA
NONNENWERTH
1000 m
N
ELANDSFONTEIN
DORSTLAND
WITRIVIER
DRENTHE
ZWARTFONTEIN
OVERYSEL
TWEEFONTEIN
SANDSLOOT
TURFSPRUIT
RIETFONTEIN
UITLOOP
OORLOGSFONTEIN
900 m
LAAGBAAN
VOLSPRUIT
10 km
30 km
50 km
70 km
iii
1,613 m
1,500 m
1,250 m
1,000 m
750 m
500 m
250 m
0 m
1000 m
VAALKOP
ii
HARRIETS WISH
AURORA
NONNENWERTH
N
ELANDSFONTEIN
DORSTLAND
WITRIVIER
ZWARTFONTEIN
TWEEFONTEIN
TURFSPRUIT
UITLOOP
OORLOGSFONTEIN
LAAGBAAN
VOLSPRUIT
10 km
30 km
50 km
70 km
iv
TURFLAAGTE
671 m
625 m
500 m
375 m
250 m
125 m
0 m
HARRIETS WISH
NONNENWERTH
N
ELANDSFONTEIN
WITRIVIER
ZWARTFONTEIN
TWEEFONTEIN
TURFSPRUIT
UITLOOP
OORLOGSFONTEIN
LAAGBAAN
VOLSPRUIT
VAALKOP
10 km
30 km
50 km
70 km

B

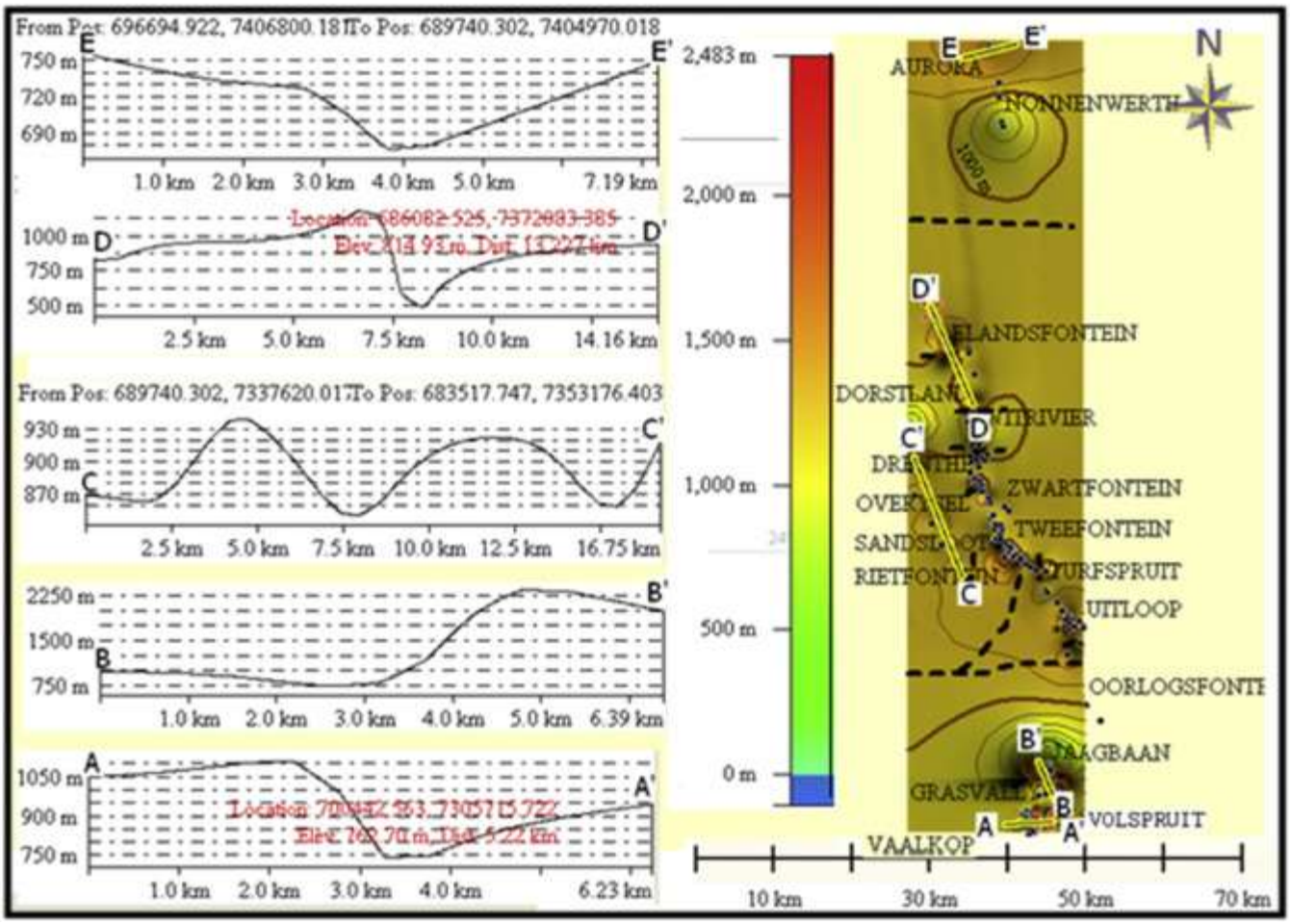
From Pos: 696694.922, 7406800.181To Pos: 689740.302, 7404970.018
E
E'
750 m
720 m
690 m
1.0 km 2.0 km 3.0 km 4.0 km 5.0 km 7.19 km
1000 m
D
D'
750 m
500 m
2.5 km 5.0 km 7.5 km 10.0 km 14.16 km
From Pos: 689740.302, 7337620.017To Pos: 683517.747, 7353176.403
930 m
900 m
870 m
C
C'
2.5 km 5.0 km 7.5 km 10.0 km 12.5 km 16.75 km
2250 m
1500 m
750 m
B
B'
1.0 km 2.0 km 3.0 km 4.0 km 5.0 km 6.39 km
1050 m
900 m
750 m
A
A'
1.0 km 2.0 km 3.0 km 4.0 km 6.23 km
2,483 m
2,000 m
1,500 m
1,000 m
500 m
0 m
AURORA
NONNENWERTH
ELANDSFONTEIN
DORSTLAND
TIRIVIER
DRANTHEM
ZWARTFONTEIN
TWEEFONTEIN
TURFSPRUIT
UITLOOP
OORLOGSFONTE
LAAGBAAN
GRASVALLEI
VOLSPRUIT
VAALKOP
N
10 km
30 km
50 km
70 km

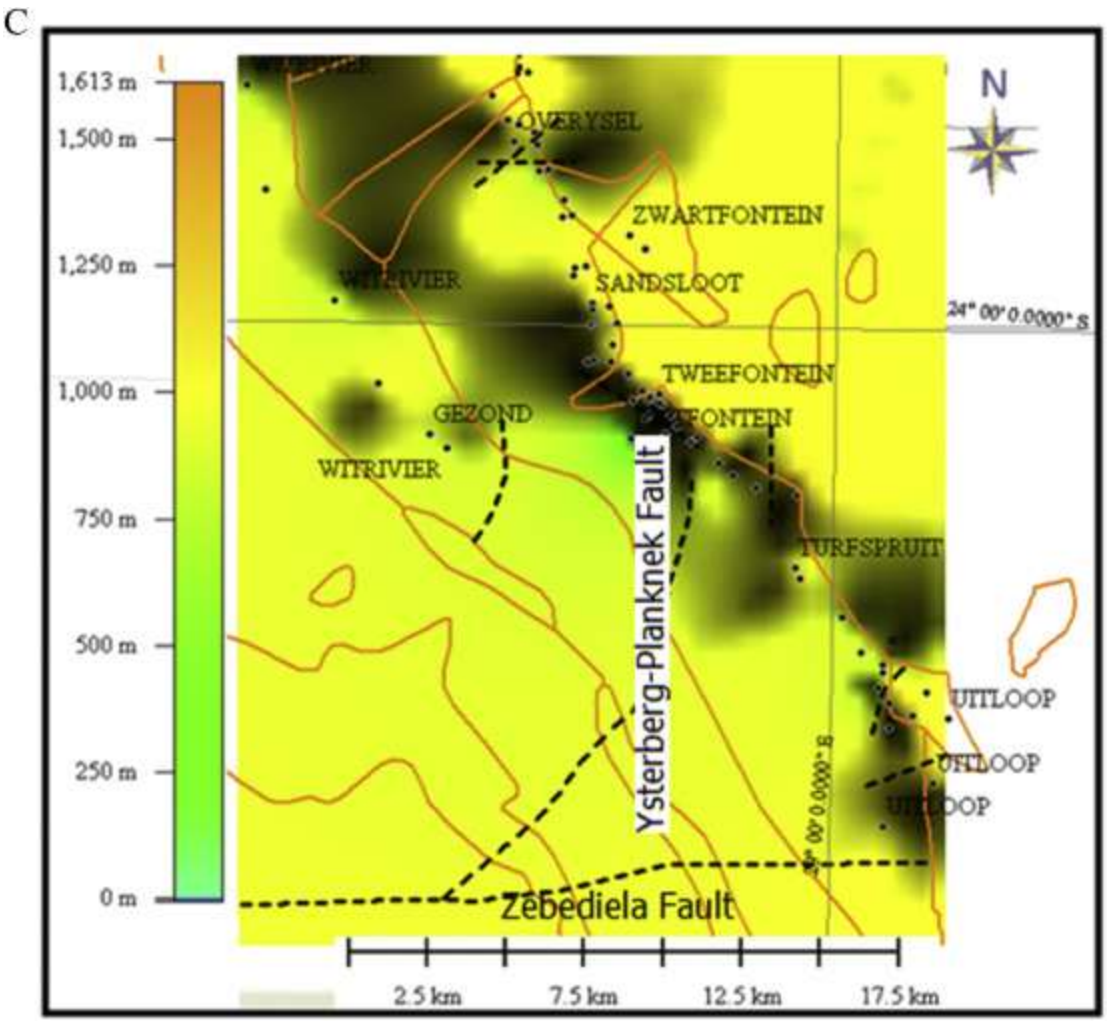

Fig. 20.
A: Diagram showing structure contour maps with inferred faults within the Northern Bushveld Complex. (i) represents some of the inferred faults in Archean floor rocks, (ii) represents the inferred faults in the Marginal Zone unit and (iii) represents the faults in the Main Zone unit, while, (iv) is the Main Zone interval isopach map.
B: Structural map of the Marginal Zone interval with profiles across some of the inferred fault planes in the Northern Buhveld Complex.
C: Close-up view of inferred faults around Overysel and Uitloop farm (A).

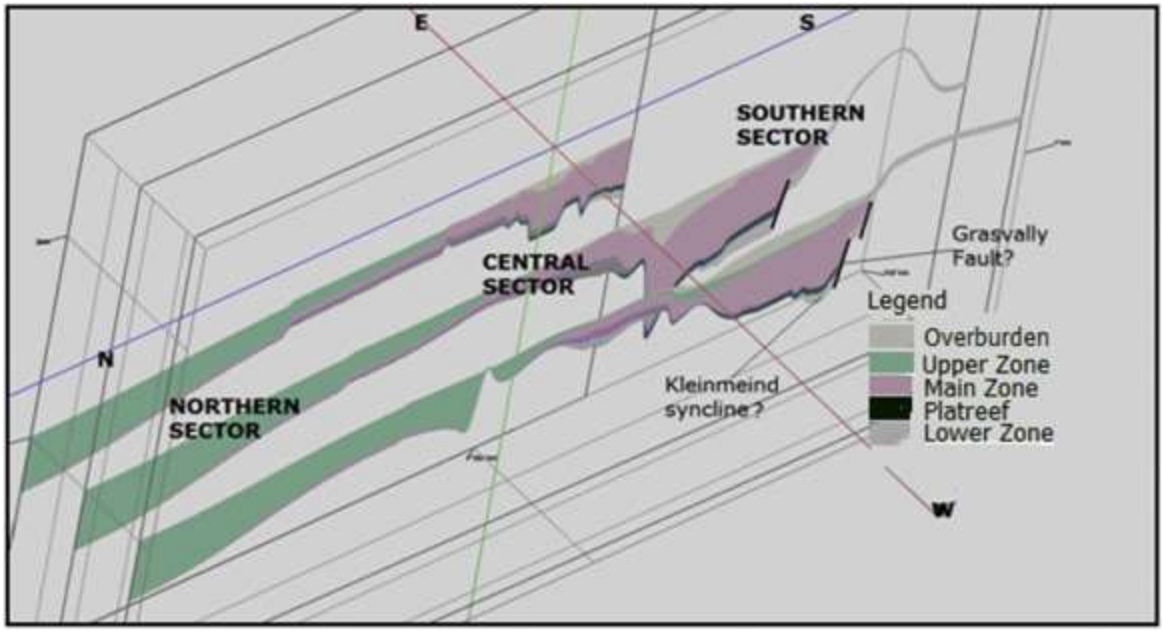

Fig. 21.
Fence diagram showing the N-S cross-sections of the Northern Bushveld Complex.

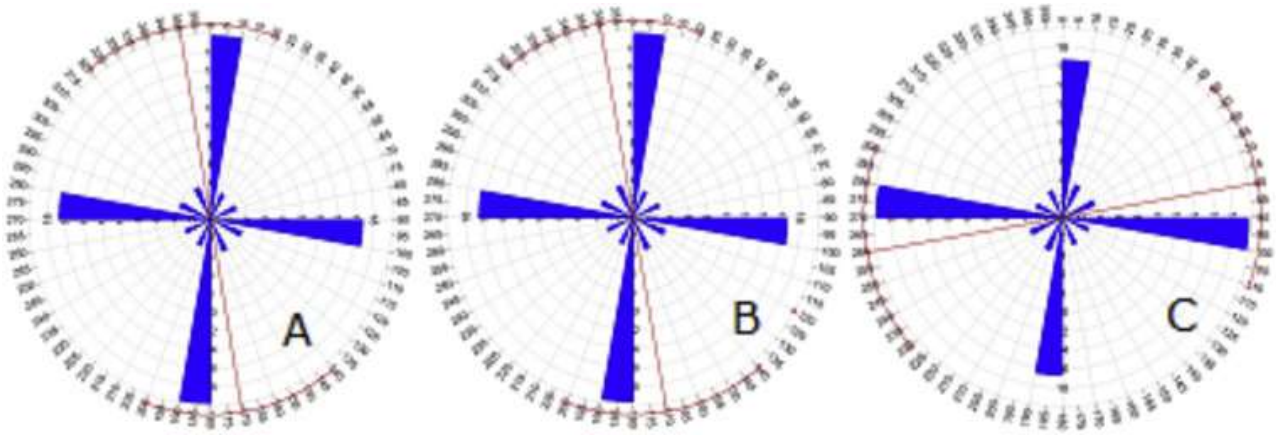

Fig. 22.
Rose diagrams showing structural trend on Upper Zone (A), Main Zone (B) and Archean rocks (C) of the northern sector of the Northern Bushveld.

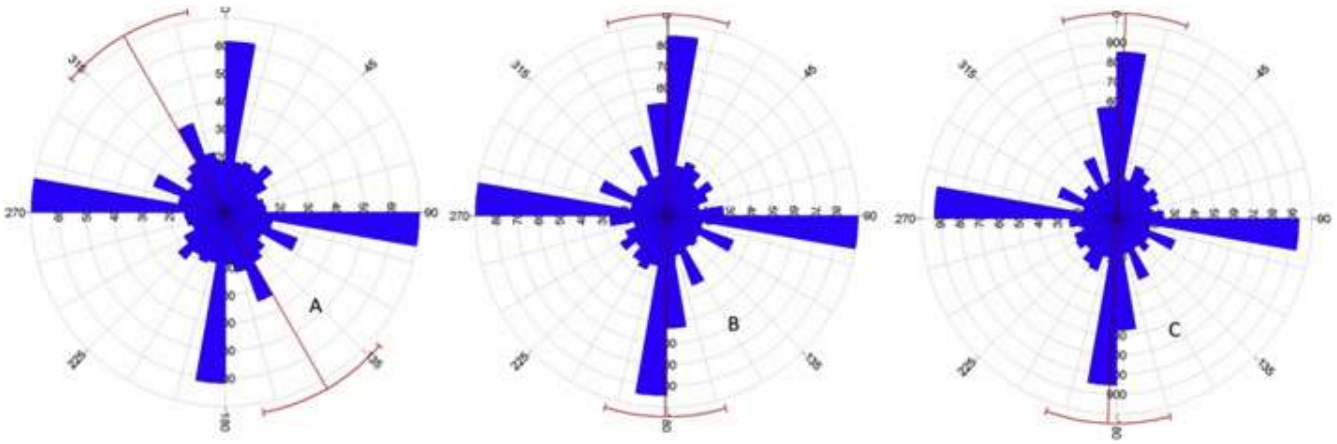

Fig. 23.
Rose diagrams of the central sector of the Northern Bushveld showing the prominent structural trend on Upper Zone (A), Lower Zone (B) and Archean rock (C).

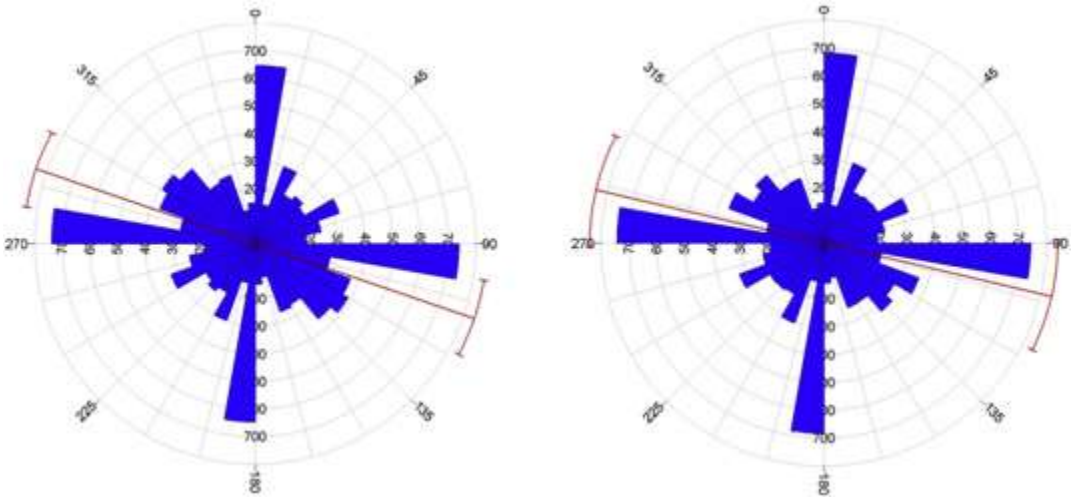

Fig. 24.
Rose diagrams showing the structural trend for the Lower Zone interval (A) and Archean rocks interval (B) in the southern sector of the Northern Bushveld.

5. Discussion

Most of the results correspond with existing geological knowledge and provide better insight on regional and local scales. Many of the structures have been reactivated several times and the present day structures are the product of a long kinematic history of over two billion years. Some of this complex fault history has been clarified. The major trends within the study area with the interpretation are given below.

- Loss of ground which is closely associated with faults and dykes (Campbell, 2009; 2011) can be related to areas where a reef is missing or normal reef trend is disturbed (Viljoen and Schurmann, 1998). Most of the inferred faults and shear zones can be categorized as areas with loss of ground.
- The Eastern Bushveld Complex is marked by irregular undulation caused primarily by faulting, folding and doming in the floor rocks.
- Du Plessis and Walraven (1990) emphasised the influence of the ENE-WSW trending Thabazimbi Murchison Lineament (TML) on the emplacement and subsequent deformation of the Bushveld Complex. NW trending structural features in the Western Bushveld include the Rustenburg Fault and fold axes in Transvaal Supergroup floor rocks. Hence, the strong ENE-WSW and NE-SW trend within the Bushveld Complex is attributed to the re-orientation of the stress field after the formation of the TML (Uken, 1999). Du Plessis and Walraven (1990) also gave a summary of the stress fields and sequence of associated motion along the TML, as reported by Coomber (2009). A major stress field identified in their study includes the E-W compressive stress (related to the Kheis orogeny (Silver et al., 2004)); NW-SE compressive force occurred during the Magondi orogeny which led to the collision of rift zones and subsequent intrusion of the Bushveld Complex. However, geochronology does not support the Kheis and Magondi Belts being coeval and the former appears to have influenced Bushveld intrusion (McCourt et al., 2001). NNW compressive force controlled the initiation of the RLS along some zones of weakness; NE-SW compressional force resulted in consequent folding with NW trending fold axes (Bumby et al., 1998). Some schools of thought (Friese, 2004; Kruger, 2005; Kinnaird, 2005) suggested that the Bushveld Complex

magmas utilized the TML, the Palala Shear Zone and the Barberton-Magaliesberg Lineaments as conduits, while the prevalent magmatic pressure and lithostatic pressure facilitated the horizontal spread of magma as sills (Silver et al., 2004). Similarly, strong control of lithospheric stress and the presence of pre-existing weak zones (shear zones) must have influenced the emplacement of the Complex.

- The structural trend around the northern sector of the Northern Bushveld includes NE-SW, NNW-SSE, ENE, and E-W directions. A N-S trend is prominent around the central part of the Northern Bushveld while NNE, WSW, and E-W trends dominate the southern sector. Friese (2004) described the NW-SE trending faults as being associated with ENE trending regional folds as thrust faults. NW trending extensional faults were associated with the Murchison Orogeny, while ENE-NNE trending strike-slip, layer parallel thrusts were interpreted as a Bushveld tectonic event. Other structural trends described by Friese (2004) include N-S extensional faults, with imbricate geometry and duplexes, and WNW to WSW trending extensional fractures identified as the youngest population of structures in the area.

6. Conclusions

In conclusion, the ability of this study to compare the geometry and trend of each stratigraphic interval structure contour map with the equvalent isopach maps, has helped in distingushing structures that were already in place before magma influx from those that formed later. This paper has been able to highlight faults constrained from geostatistical analysis to substantiate the existence of some previously identified faults, fault related features and to elucidate their geometry at the subsurface. It also shows a new way of mapping subsurface geological features in detail. It allows better understanding of local and regional structural trends and the geometry of the inferred structures. Consequently, previously unsubstantiated inferences or assumptions about the RLS subsurface structures and the floor rock became conclusively evident, while

additional information was also added to the existing detail. Major advantages of this study also include the excellent conformity of the results with previous field studies and geophysical investigation. A summary of the major structural trends and their interpretations is given in Table 1.

Table 1.

Prominent structural trends in this study

Part of BC	Upper Zone	Main Zone	Lower Zone	Marginal Zone	Archaean basement	Structural trends and interpretation
Amandelbult section of Northwestern Bushveld	NNW, NW	NE-SW, NNE, ENE, NS, E-W	NNE, NE-SW, NS, ENE			The NE-SW trend bifurcates the NNW trend and might be younger than the latter. The NE-SW trend is prominent on the Main Zone and lower stratigraphic horizons.
Northwestern Bushveld (north of Pilanesberg complex)	ENE-WSW NNWNNE, NE-SW, NW,	NW-SE, NNW, NE-SW, E-W, NS	NW-SE, NNW, NE-SW, N-S, E-W			The NW trend is more dominant along the gap areas, it represents the presence of NW trending faults.
South of Pilanesberg Complex (central parts of Western BC)	NNE, WSW NNW, NW	NNE, WSW NNW, NW	NNE, WSW NNW, NW	NNE, WSW NNW, NW		Faults around the Pilanesberg Complex trend mostly NW-SE, NE-SW, NNE and WNW, are said to be post Bushveld and probably due to the emplacement of the Alkaline Complex. Trend of the Rustenburg Fault is NW. Eastward from the Rustenburg fault are NW trending fold axes also parallel to the trend of the Rustenburg Fault

Part of BC	Upper Zone	Main Zone	Lower Zone	Marginal Zone	Archaean basement	Structural trends and interpretation
Southwestern BC	NE-SW, NW-SE, NNE, N-S,	NNW, WNW, NS, E-W	E-W, NE-SW, NW, N-S,	E-W, NE-SW NW,	E-W, , NE-SW NW,	The area is dominated by NW to NNW trends around the Brits graben.
Northeastern BC	WNW, NNW,NNE, N-S, NE-SW,	N-S, NNW, NNE	N-S, NNW, NNE			The N-S structural trend in this area coincides with the trend of the periclines in the floor of the BC (Uken, 1998) and are influenced by the emplacement of the RLS. Most of the faults in this area (the Wonderkop Fault, the Stofpoort fault and the Sekhukhune) trend N-S, NNW and NNE
Southeastern BC	NNW, NNE, NW-SE, E-W, NE-SW	NNW, NW, N-S, NNE, E-W, ENE	NNW,NW, N-S, NNE, E-W, ENE			Main structural trend is NNW. This coincides with the trend of Laersdrift fault in the southeastern part of the Eastern Bushveld Complex

Part of BC	Upper Zone	Main Zone	Lower Zone	Marginal Zone	Archaean basement	Structural trends and interpretation
Northern sector of the Northern BC	NNE, WNW,	NNE, WNW,			NNE, WNW	Structures in the floor rock influenced the geometry of the RLS rock in most parts of the northern BC. Prominent trends identified within the northern BC coincide with the faults already identified by Friese (2004) and subdivided into the following

						(from oldest to youngest);(i)The ENE trending thrust faults (ii) The NW-WNW trending extensional faults probably developed during the Murchison Orogeny, (iii) The ENE-NNE dextral stike-slip Faults that developed during the Limpopo orogeny and reactivated during the BC emplacement (Armitage, 2011) (iv) N-S extensional faults, (v) WNW to WSW extensional fractures identified as the youngest population of structures in this area.
Part of BC	Upper Zone	Main Zone	Lower Zone	Marginal Zone	Archaean basement	Structural trends and interpretation
Central sector of the Northern BC	WNW, NNE, NW,NNW,		NNE, N-S, NNW,		WNW, N-S, NNW,	
Southern sector of the Northern BC			NNE, WNW,		NNE, WNW,	

Acknowledgements

The authors appreciate the management of the Council for Geosciences Pretoria, South Africa for granting access to borehole data, software facilities and other relevant information. The University of Pretoria and the Federal University of Technology, Akure through the ETF initiative is appreciated for financial support.

REFERENCES

Armitage, P. E. B., 2011. Development of the Platreef in the northern limb of the Bushveld Complex at Sandsloot, Mokopane District, South Africa. PhD thesis University of Greenwich. 284pp.

Barclay, J., Krause, F., Campbell, R., Utting, J., 1990. Dynamic casting and growth faulting: Dawson Creek graben complex, Carboniferous-Permian Peace River embayment, western Canada. Bulletin of Canadian Petroleum Geology, 38**,**115-145.

Blaine, J.L., 1973. Report on the Potgietersrus project, Potgietersrus, Northern Transvaal. Internal report 1323. Falconbridge, Toronto.

Bumby, A., Eriksson, P.G., Van Der Merwe, R., 1998. Compressive deformation in the floor rocks to the Bushveld Complex (South Africa): evidence from the Rustenburg Fault Zone. Journal of African Earth Sciences, 27**,** 307-330.

Campbell, G., 2006. High resolution aeromagnetic mapping of "loss-of-ground" features at platinum and coal mines in South Africa. South African Journal of Geology, 109, 439-458.

Campbell, G., 2009. Seismic reflection surveys and structural mapping: Faults,dips and domes. 11th SAGA Biennial Technical Meeting and Exhibition Swaziland.

Campbell, G., 2011. Exploration geophysics of the Bushveld Complex in South Africa. The Leading Edge, 30**,** 622-638.

Cant, D.J., 1988. Regional structure and development of the Peace River Arch, Alberta: a Paleozoic failed-rift system? Bulletin of Canadian Petroleum Geology, 36, 284-295.

Cather, S.M., Harrison, R.W., 2002. Lower Paleozoic isopach maps of southern New Mexico and their implications for Laramide and ancestral Rocky Mountain tectonism. 53rd Annual Field Conference Guidebook, 2002. 85-101.

Clarke, B.M., Uken, R., Watkeys, M.K., Reinhardt, J., 2005. Folding of the Rustenburg layered suite adjacent to the Steelpoort pericline: implications for syn-Bushveld tectonism in the eastern Bushveld Complex. South African Journal of Geology, 108, 397-412.

Clarke, B., Uken, R., Reinhardt J., 2009. Structural and compositional constraints on the emplacement of the Bushveld Complex, South Africa. Lithos. 111, 21-36.

Cole, J., Finn, C.A., Webb, S.J., 2013. Overview of the magnetic signatures of the Palaeoproterozoic Rustenburg Layered Suite, Bushveld Complex, South Africa. Precambrian Research, 236, 193-213.

Coomber, S.J., 2009.Gravity modelling in the western Bushveld Complex, South Africa, using integrated geophysical data. MSc thesis University of Witwatersrand, Johannesburg. url:http://hdl.handle.net/10539/6962.

Du Plessis, A., Levitt, J.G., 1987. On the structure of the Rustenburg layered suite—insight from seismic reflection data. Indaba on the tectonic setting of layered intrusives, Geol. Soc. of Africa, Pretoria, 14-15.

Du Plessis, A., Kleywegt, R..J., 1987. A dipping sheet model for the mafic lobes of the Bushveld Complex. South African journal of geology, 90, 1-6.

Du Plessis, C., Walraven, F., 1990. The tectonic setting of the Bushveld Complex in Southern Africa, Part 1. Structural deformation and distribution. Tectonophysics, 179**:** 305-319.

Friese, A.E.W., 2004. Geology and tectono-magmatic evolution of the PPL concession area, Villa Nora-Potgietersrus Limb, Bushveld Complex. Geological Visitor Guide, Potgietersrus Platinums Limited, 57.

Friese A.E.W., Chunnett, G., 2004. Tectono-magmatic development of the northern limb of the Bushveld Igneous Complex, with special reference to the mining area of Potgietersrus Platinums Limited. Geoscience Africa 2004 Abstract Volume, Johannesburg**,** 209-210.

Groshong Jr, R.H., 2006. 3D Structural Geology–A Practical Guide to Quantitative Surface and Map Interpretation. Springer.411pp.Jones, J., Sudicky, E., Mclaren, R., 2008. Application of a fully-integrated surface-subsurface flow model at the watershed-scale: A case study Water Resources Research, 44.

Hulbert L.J., 1983. A petrographical investigation of the Rustenburg Layered Suite and associated mineralization south of Potgietersrus. Unpublished DSc dissertation, University of Pretoria, 511 pp.

Kinnaird, J.A., 2005. The Bushveld large igneous province. Review Paper, The University of the Witwatersrand, Johannesburg, South Africa, 39pp.

Kruger, F. J., 2005. Filling the Bushveld Complex magma chamber: lateral expansion, roof and floor interaction, magmatic unconformities, and the formation of giant chromitite, PGE and Ti-V-magnetitite deposits. Mineralium Deposita, 40**,** 451-472.

Meyer, R., De Beer, J.H., 1987. Structure of the Bushveld Complex from resistivity measurements. Nature 325, 610–612.

McCourt, S., Hilliard, P., Armstrong, R.A., Munyanyiwa, H., 2001. SHRIMP U-Pb zircon geochronology of the Hurungwe granite northwest Zimbabwe: Age constraints on the timing of the Magondi orogeny and implications for the correlation between the Kheis and Magondi Belts. South African Journal of Geology, 104(1), 39-46.

Mei, S., 2009. Geologist-controlled trends versus computer-controlled trends: introducing a high-resolution approach to subsurface structural mapping using well-log data, trend surface analysis, and geospatial analysis. Canadian Journal of Earth Sciences, 46**,** 309-329.

Mossop, G.D., Shetsen, I.,1994.Geological atlas of the Western Canada sedimentary basin, Alberta Research, Council Canadian Society of Petroleum Geologists, Published jointly by the Canadian Society of Petroleum Geologists and the Alberta Research Council.

Nex, P.A., 2005. The structural setting of mineralisation on Tweefontein Hill, northern limb of the Bushveld Complex, South Africa. Applied Earth Science: Transactions of the Institutions of Mining and Metallurgy: Section B, 114, 243-251.

Odgers, A.T.R., 1998. Structure of the southern Bushveld Complex as determined from regional reflection seismic: South African Geophysical Reviews, v. 2.79-82.

Odgers, A.T.R., Hinds, R.C., Von Gruenewaldt, G., 1993. Interpretation of a seismic reflection survey across the southern Bushveld Complex. South African journal of geology, 96, 205-212.

Paulson, O. L., Peascatore F.T., 1979. The Effects of the Phillips Fault Zone on Subsurface Jurassic Sediments and Petroleum Production of Jasper County, Mississippi. Mississippi Mineral Resources Institute, University of Mississippi, no 792, 15pp

Perritt, S., Roberts, M., 2007. Flexural-slip structures in the Bushveld Complex, South Africa?. Journal of Structural Geology, 29, 1422-1429.

Prost G.L., 2004. Tectonics and hydrocarbon systems of the East Gobi basin, Mongolia. AAPG bulletin, 88**,** 483-513.

Roberts, L.N., 2003. Structure contour map of the top of the Dakota Sandstone, Uinta–Piceance Province, Utah and Colorado. Petroleum Systems and Geologic Assessment of Oil and Gas in the Uinta–Piceance Province, Utah and Colorado: US Geological Survey, Digital Data Series DDS–69–B.

Silver, P.G, Fouch, M.J., Gao, S.S., Schmitz, M., 2004. Seismic anisotropy, mantle fabric, and the magmatic evolution of Precambrian southern Africa. South African Journal of Geology, 107**,** 45-58.

Trickett, J.C., Duweke, W., Kock, S., 2005. Three-dimensional reflection seismic: worth its weight in platinum. SAIMM Journal of the South African Institute of Mining and Metallurgy, 105, 357 -363.

Uken, R., Watkeys, M.K., 1997. An interpretation of mafic dyke swarms and their relationship with major mafic magmatic events on the Kaapvaal Craton and Limpopo Belt. South Afr. J. Geol., 100**,** 341-348.

Uken, R., 1999. The geology and structure of the Bushveld Complex metamorphic aureole in the Olifants River area. University of Natal, Durban, South Africa, 277 pp.

Van Der Merwe, M.J., 1978. The geology of the basic and ultramafic rocks of the Potgietersrus limb of the Bushveld Complex (Doctoral dissertation, Universityof The Witwatersrand. Typescript (Photocopy). Contains 4 Maps In Back Pocket.).

Van Der Merwe, M.J., 2008. The geology and structure of the Rustenburg Layered Suite in the Potgietersrus/Mokopane area of the Bushveld Complex, South Africa. Miner. Deposita, **43**, 405-419.

Vermaak C.F .1976. The Merensky Reef; thoughts on its environment and genesis. Econ Geol 71:1270–1298

Viljoen, M. J., Schurmann LW. 1998. Platinum-Group Metals. In: Wilson, M. C. G. & Anhaeusser, C. R. (eds.) The Mineral Resources of South Africa. Council for Geoscience, Pretoria, South Africa. pp 532-568.

Xu, S.-S, Velasquillo-Martinez, L.G., Grajales-Nishimura, J.M., Murillo-Muñetón, G., García-Hernández, J., Nieto-Samaniego, A.F., 2004. Determination of fault slip components using subsurface structural contours: methods and examples. J. Petrol. Geol, 27, 277-298.